Office of Surface Mining Reclamation and Enforcement (OSMRE)
Cooperative Agreement S23AC00043-00

Final Report: January 1, 2023, to December 31, 2024

Title: Optimizing rare earth element capture during treatment of acid mine drainage: validation of geochemical modeling through bench-scale experiments and proof-of-concept field studies

PI: Brian W. Stewart, University of Pittsburgh
Co-PIs: Rosemary C. Capo, University of Pittsburgh
Charles A. Cravotta III, U.S. Geological Survey, retired; Cravotta Geochemical Consulting
Benjamin C. Hedin, Hedin Environmental

Technical point of contact: Dr. Brian W. Stewart
Department of Geology & Environmental Science
University of Pittsburgh
200 SRCC
Pittsburgh, PA 15260
Telephone: 412-624-8780
Email: bstewart@pitt.edu

Project dates: January 1, 2023 – December 31, 2024

1. Overview

The goal of this project was to develop and test a scalable method for efficient extraction of rare earth elements and yttrium (REY) from acidic mine drainage (AMD). Work on this project included (1) development of a modeling framework that can accurately describe the co-precipitation and adsorption of REY with solid phases (mineral and amorphous) that are formed when coal AMD of variable composition is neutralized; (2) validation of specific model predictions using benchtop batch precipitation/adsorption experiments on simulated AMD; (3) development and initial testing of a field-based flow-through system in Al-rich and Mn-rich high-REY AMD in order to better understand the nature of economic concentrations of REY and other critical metals at or near the discharge source; and (4) dissemination of these findings to AMD stakeholders and the greater scientific community, in part via presentations at conferences and publication in peer-reviewed journals, and integration into an innovative geochemical modeling tool (PHREEQ-N-AMDTreat), which can provide immediate on-the-ground resources for end users by providing cost-benefit analysis and treatment strategies for REY recovery.

This project was a collaborative effort involving expertise in coal mine drainage, laboratory experiments, geochemical analysis, and geochemical modeling from University of Pittsburgh, USGS, and Hedin Environmental investigators. Building on our team's previous work, we carried out a suite of new bench-

top experiments combined with geochemical equilibrium modeling to better determine treatment conditions (*e.g.*, pH, redox, metals and ligand concentrations) under which precipitation of solids can be achieved while concentrating REY removal at specific steps. A PHREEQC equilibrium model was applied to identify potential interactions during the precipitation of solids, including those containing REY, the distribution of aqueous and surface (sorption) species of REY and associated ions, and the sorbent composition and mass. Batch titration experiments were used to evaluate the potential for REY coprecipitation with manganese and aluminum and to determine REY adsorption parameters on precipitated AMD minerals. Model calibration based on the experimental results was used to determine optimum conditions for the efficient precipitation of target and non-target solids. These experiments and modeling were validated using AMD collected from two remediation sites. This combined and, most importantly, iterative experimental and modeling approach evaluating a wide range of variables can aid in the design of an up-scalable modular, retrievable REY-capture device that can be implemented in field testing of REY capture and recovery.

The modeling, experiments, and technology demonstration from this project can result in improved engineering designs that target REY recovery and provide additional economic incentive for AMD treatment of impacted streams. Integration of results into the AMDTreat water-quality modeling tool (PHREEQ-N-AMDTreat) provides end-users the ability to up-scale results to field application and aid in cost estimates on the scale of individual AMD discharges. In addition, results have been disseminated via scientific publications and meeting presentations. This project also involved the training of a Ph.D. graduate student in geochemical modeling, bench-top experimental techniques, and AMD remediation.

The modeling and experiments provide guidance for selective precipitation of major dissolved metal components in Appalachian AMD, with possible application to other types of mine drainage, which can help optimize both active and passive treatment systems. This project focused on the most environmentally damaging low-pH mine drainage systems that have highest concentrations of REY, making treatment of these discharges more feasible. Calculations for scaling up the treatments to the level of individual discharges provide mine drainage remediation operators the ability to determine whether and when it could be advantageous to incorporate REY recovery into treatment systems. Calculations of REY recovery and scale-up cost allow implementation of the recovery system when the economics are most advantageous, *e.g.*, after geopolitical disruption of normal supplies.

Deliverables

Deliverables include the following: (1) a final report following OSMRE guidelines, available in electronic form; (2) a written summary or fact sheet in the appropriate OSMRE format; (3) a PowerPoint presentation at a technical event (*e.g.*, the WVMD Task Force) summarizing the work completed at the appropriate level; (4) electronic copy of peer-reviewed abstracts and an articles resulting from the proposed research; (5) additional technology transfer as outlined in the results from Task 7.

2. Project Results

The proposed work focused on REY extraction from AMD, with the goal of producing solids from which REY can be efficiently and economically recovered. The knowledge gaps addressed include (1) partitioning of REY among solution complexes and one or more solid phases in precipitating AMD fluids; (2) the precise mechanism by which REY are captured by precipitating phases in AMD; (3) the extent to which AMD can be manipulated to maximize REY capture at the highest possible

concentrations while maintaining its characteristic enrichment of the most critical REY; (4) the extent to which REY can be captured in a solid that allows efficient REY remobilization during processing; (5) the ability of equilibrium geochemical models to predict REY behavior in complex AMD-type fluids.

This project builds on previous research and expertise in the enrichment and sequential extraction of critical metals (especially REY) in AMD remediation systems (Cravotta, 2008a; 2008b; Stewart et al., 2017; Hedin et al., 2019; 2020; 2024) to address the following important questions:

(1) Can we identify conditions where REY (or specific members of the group, for that matter) are primarily attenuated by Al versus Mn oxyhydroxides?

(2) Are simple adjustments to pH and ionic composition sufficient to affect these distributions?

(3) Are the REY incorporated in mineral structures as solid solutions or adsorbed on surfaces?

(4) Once extracted to the solids, what effort/process may be involved to recover the REY and possibly reuse the solids to better concentrate REY?

Knowledge gaps addressed by this project include:

(1) Partitioning of REY among solution complexes and one or more solid phases in precipitating AMD fluids; (2) the precise mechanism by which REY are captured by precipitating phases in AMD; (3) the extent to which AMD can be manipulated to maximize REY capture at the highest possible concentrations while maintaining its characteristic enrichment of the most critical REY; (4) the extent to which REY can be captured in a solid that allows efficient REY remobilization during processing; (5) the ability of equilibrium geochemical models to predict REY behavior in complex AMD-type fluids.

Our results have been integrated into an innovative geochemical modeling tool (PHREEQ-N-AMDTreat+REYs) to guide users in the construction of AMD remediation systems that optimize REY recovery.

The two-year project, which began January 2023, was divided into seven tasks (Table 1). The sections that follow delineate the results of each task.

2.1 Task 1: Initial PHREEQc Predictive Models

To evaluate the relative importance of different variables on the sequestration and recovery of REY from AMD, a geochemical equilibrium model using PHREEQC (Parkhurst and Appelo, 2013) with an expanded thermodynamic "wateq4fREYsKinetics.dat" database was further developed, validated, documented, and released as a project deliverable.

Specific related milestones achieved for this task:

a. The original PHREEQ-N-AMDTreat+REYs equilibrium-adsorption models described in Cravotta (2021a) were expanded to include the potential precipitation of various REY-solids including oxalate, phosphate, and carbonate compounds as well as selected La-Ce phosphate, carbonate, or hydroxide solid solutions that may form during conventional treatment or specialized treatment to recover REY. Additionally, three new models that include adsorption of REY by humic acid (HA) were added to the suite of tools -- CausticTitrationMix2REYsKineticsHA, CausticTitrationMix2REYsKineticsMolesHA,

Table 1. Task chart for the project showing final completion dates of milestones. It was determined that column experiments (Milestones 2b and 3c) were not required to achieve the program objectives.

Task Name and Milestone	Assigned Resources*	YEAR 1 (2023)				YEAR 2 (2024)			
		Q1	Q2	Q3	Q4	Q5	Q6	Q7	Q8
Task 1. Initial PHREEQC predictive models	**CGC, Pitt**								
Milestone 1a. Add solid sol'n to model/database									
Milestone 1b. Add REY sorption reactions to data base									
Milestone 1c. Add surface area/density as parameters									
Task 2. Determine experiment parameters	**CGC, Pitt**								
Milestone 2a. Determine synthetic AMD compositions									
Milestone 2b. Obtain/synthesize sorbent minerals									
Milestone 2c. Plan sequence steps and conditions									
Milestone 2c. Compile/construct experiment apparatus									
Task 3. Precipitation/adsorption experiments	**Pitt**								
Milestone 3a. Determine blanks									
Milestone 3b. Complete initial set of batch experiments									
Milestone 3c. Complete column experiments									
Task 4. Constrain geochemical models	**CGC, Pitt, HE**								
Milestone 4a. Adjust database based on experiments									
Milestone 4b(1). Refined models to reflect observations									
Milestone 4b(2). Incorporate bench-scale datasets									
Milestone 4b(3). Develop model documentation/instructions									
Milestone 4c. Use models to optimize REE recovery									
Task 5. Proof-of-concept field tests	**Pitt, HE, CGC**								
Milestone 5a. Design proof-of-concept field unit									
Milestone 5b. Emplace and monitor field unit									
Milestone 5c. Analyze/evaluate performance of field unit									
Task 6. Scaling up calculations	**Pitt, HE, CGC**								
Milestone 6a. Calculate parameters for discharge scale									
Milestone 6b. Calculate cost/return of scaled-up recovery									
Task 7. Technology transfer	**Pitt, CGC, HE**								
Milestone 7a. Submit manuscripts on results and REY capture									
Milestone 7b. Present results at technical meetings									
Milestone 7c. Modeling parameters available on website									
Milestone 7d. Submit final report to OSMRE									

*Pitt = University of Pittsburgh; CGC = Cravotta Geochemical Consulting; HE = Hedin Environmental.

and TreatTrainMix2REYsHA. Sorbent may include HA, only, or in combination with hydrous metal oxides.

b. Rare earth element sorption reactions on hydrous manganese oxides (HMO) and hydrous aluminum oxides (HAO) were updated in the wateq4fREYsKinetics database (Milestone 1b) following benchtop experiments carried out by graduate student Tashane Boothe-Lordon on synthesized HMO and HAO. Updated constants for HAO-REY adsorption based on HCl and H_2SO_4 experiments of Boothe-Lordon, which consider sorption over a range of SO_4 concentrations (0 to 2900 mg/L) characteristic of AMD systems, supersede previous values from Tasker et al. (2025).

c. Sorbent surface area and site density properties for existing or freshly precipitated sorbent were added as adjustable parameters on the user interface. Two different case-study examples using bench-scale datasets for titration of real AMD (Kentucky Hollow) or cubitainer kinetic tests of AMD reaction rates

with limestone or steel slag and associated attenuation of dissolved metals, including REYs (Portage Railroad) were used as validation.

The geochemical modeling tools account for the variable pH and redox conditions in untreated AMD or treated effluent at points within a passive or active AMD treatment system. At each pH step (titration model) or time step (sequential model), REY distributions and compositions of the solids, and corresponding interactions between the aqueous species and solid phases, are computed. The updated PHREEQ-N-AMDTreat+REYs models (version 1.0.6) were made available to project collaborators and released to the public during year 2 by Co-PI C. Cravotta.

The PHREEQ-N-AMDTreat+REYs models developed in Task 1were used by graduate student Tashane Boothe-Lordon to determine parameters (solute concentrations, pH ranges, sulfate levels) for planning of the bench-scale adsorption experiments (Task 2). The data from these experiments were fed back to further constrain the geochemical models (Task 4) Documentation and instructions for utilization of the PHREEQ-N-AMDTreat+REYs models were developed and made available to the public via a workshop at the 2024 International Mine Water Association Conference (Task 7) (PHREEQ-N-AMDTreat model to evaluate water-quality effects from passive and active treatment of mine drainage - WVTF | IMWA 2024). The current version 1.0.6 will be provided to another group of workshop participants at the 2025 IMWA conference, PHREEQ-N-AMDTreat - IMWA 2025 | Portugal & Spain.

2.2 Task 2: Determine experiment parameters.

Based on the results of the initial equilibrium modeling and an evaluation of Appalachian coal mine drainage geochemical data (e.g., Cravotta, 2008a; 2008b; Cravotta and Brady, 2015), the team developed and implemented a plan for precipitation and adsorption experiments to determine the extent to which specific REY are adsorbed/co-precipitated with different solids. Milestones achieved for this task included (1) the determination of appropriate endmember AMD compositions for the production of synthetic AMD fluids that provide representative samples of Appalachian coal mine drainage; (2) the sequence of treatments to change pH/redox and sequentially precipitate solids and co-precipitate or adsorb REY; (3) volumes of starting material and additives, including possible spiking with REY, to allow for accurate representation of treatment of coal-mine fluids and precipitates to recover REY; and (4) procedures for synthesizing sorbent minerals used as reactive substrates in experiments.

For HMO: The initial experiments on critical metal capture focused on manganese oxy-hydroxides (HMO), which are a potentially major sink for rare earth elements (REE) from AMD (Hedin et al., 2019). This work leveraged earlier work by co-investigator Hedin (Hedin et al., 2024) and Ph.D. student Tashane Boothe-Lordon (Boothe-Lordon et al., in revision, 2025) by comparing abiotic critical metal uptake in Mn minerals to earlier biotic results. Ms. Boothe-Lordon developed a method to abiotically synthesize HMOs based on earlier work by Villalobos et al. (2003) and successfully generated gram quantities of HMOs that appear to be similar to δ-MnO_2 and H+ birnessite based on XRD data (Task 2, Milestone 2a, b).

For HAO: The parameters for HAO sorption and co-precipitation experiments were determined. In particular, we examined the importance of pH and aqueous concentrations of sulfate (SO_4) and aluminum on the attenuation of REE by Al hydroxide and hydroxysulfate phases such as gibbsite ($Al(OH)_3$) and basaluminite ($Al_4SO_4(OH)_{10}:5H_2O$). These phases precipitate within a pH range (4.5-6) that is commonly attained in AMD treatment systems and are important for removing SO_4, Al, and trace metals as AMD is neutralized.

2.3 Task 3: Precipitation/adsorption experiments

Experiments were carried out in the labs of PI Stewart and Co-I Capo at the University of Pittsburgh and were a primary focus of the graduate students involved in this project. Initial work, informed by the geochemical modeling, focused on the batch precipitation/adsorption experiments to determine the behavior of REY when mine waters are manipulated to precipitate solids of different compositions or to facilitate sorption of REY on specific substrates. Both the solids and fluids were analyzed for major, minor and trace elements, including REY. Milestones achieved included a) determination of blanks for experimental apparatus using pH-adjusted ultrapure water; b) completion of batch precipitation/adsorption experiments on using predicted precipitation parameters, additional leaching experiments to evaluate possible recovery of REY without dissolving sorbent, and analysis of related fluids and precipitates. Results of this work were presented at scientific meetings.

2.3.1 Hydrous manganese oxide (HMO) experiments

Graduate student Tashane Boothe completed batch experiments on adsorption of rare earth elements and yttrium (REY) by hydrous manganese oxides (HMO), a common solid in acid mine drainage (AMD) systems. These experiments were designed to evaluate the effects of biotically- versus abiotically-precipitated HMO. Results show the following: (1) Both biotic (fungal) and abiotic HMOs are effective at adsorbing REY (Fig. 1), with biotic HMO removing >99% of REY from solution after 31 days compared to 50-80% for abiotic HMO; (2) in most cases, light REY are adsorbed more efficiently than heavy REY; and (3) fungal biomass alone can effectively adsorb REY. Results from these experiments were presented by Boothe-Lordon in July 2023 at the international Goldschmidt Geochemistry Conference in Lyon, France (expenses not paid by this grant) and in 2024 at the American Chemical Society Central Regional Meeting, in Pittsburgh, Pennsylvania.

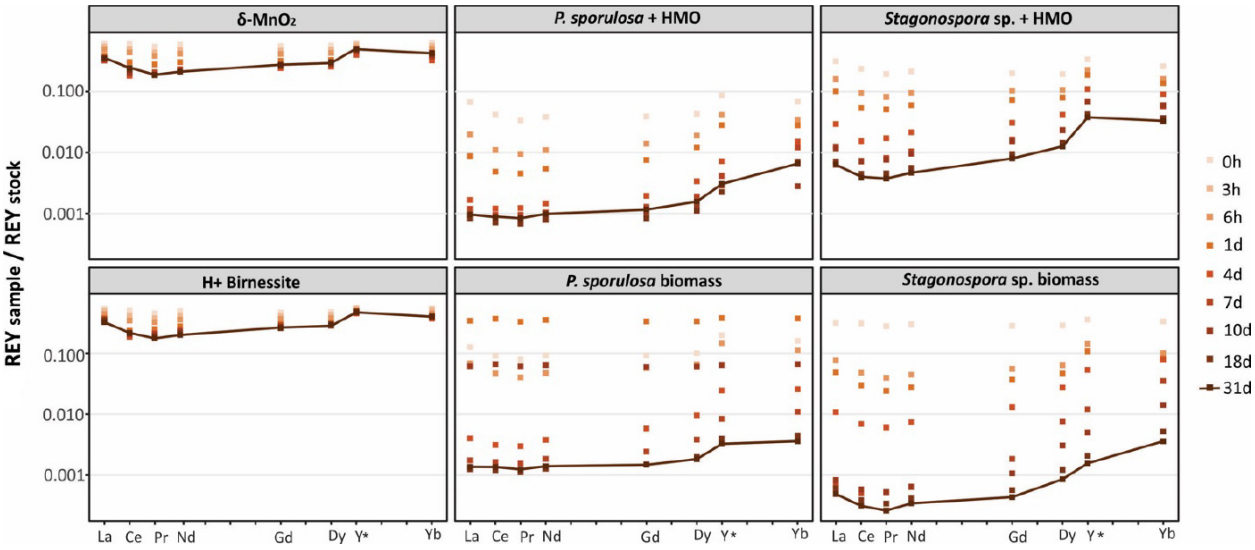

Figure 1. Results of REY adsorption experiments (1) under abiotic conditions (left plots), (2) with fungally-precipitated HMO, and (3) with fungal biomass alone. REY were adsorbed during all experiments, but those with fungi showed the greatest amount of adsorption.

Tashane Boothe-Lordon characterized the solids from her initial batch experiments on adsorption of rare earth elements (REE) by hydrous manganese oxides (HMO). X-ray diffraction (XRD) patterns (Fig. 2) shows that the initial HMO produced from the biotic experiments, sampled 6 hours after introducing critical metals to the solutions, is amorphous to weakly crystalline, indicating the presence of a poorly crystalline phyllomanganate resembling vernadite. After 31 days, the solids from the same experiments show much more defined peaks clearly resembling δ-MnO_2 (the synthetic analogue of vernadite) with symmetrical peaks at 1.4Å and 2.4Å. XRD patterns for the synthesized δ-MnO_2 (DM) and H+ birnessite (HB) are shown in red for comparison.

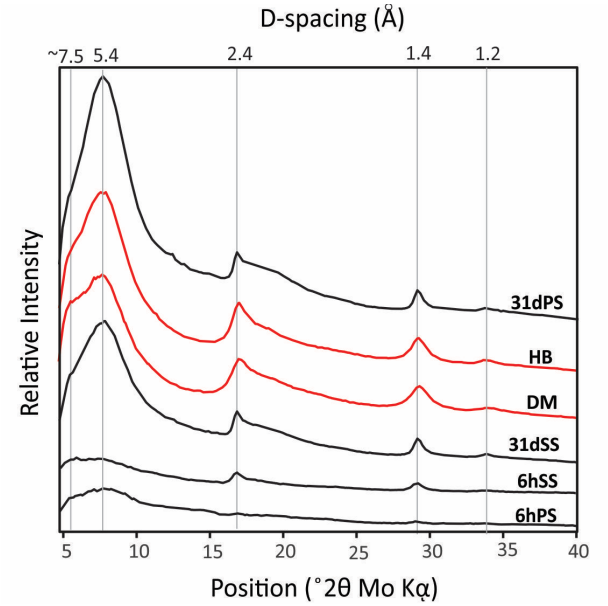

Figure 2. XRD patterns of biotic HMO produced by *Stagonospora sp*. at 6 hours (6hSS) and 31 days (31dSS) and *P. sporulosum* at 6 hours (6hPS) and 31 days (31dPS) are compared to abiotic HMO, H+ birnessite (HB) and δ-MnO_2 (DM). Note the sharpening of peaks at 2.4Å and 1.4Å for the biotic experiments over time, indicating increased crystallinity of these solids.

Experiments in which abiotic REE were added to solutions containing abiotically synthesized HMO (in the same growth medium) show that while REE are still adsorbed to a significant degree (Fig. 3a), the extent of adsorption is much less that that shown by biotic HMO (Fig. 3b). Data from these experiments are still being analyzed; one factor for the lesser extent of adsorption could be instability of HMO in the growth medium. Nonetheless, the role of microorganisms must clearly be considered when developing strategies for HMO capture of REE.

During Q4, graduate student Boothe-Lordon presented her preliminary findings at the Geological Society of American Annual Meeting in Pittsburgh, PA (Boothe TJ, Capo RC, Stewart BW, Rosenfeld CE, 2023, *A comparative assessment of critical metal removal by biotic and abiotic hydrous manganese oxides*). Additional results were presented at the Joint Conference of the West Virginia Mine Drainage Task Force Symposium and International Mine Water Association meeting held in April 2024 (Boothe TJ, Capo RC, Stewart BW, Hedin BC, Olds TA, Rosenfeld CE, 2024, *Lab-based assessment of critical metal adsorption by biotic and abiotic hydrous manganese oxides*).

A paper presenting these results is currently under review for the American Chemical Society journal *ACS Omega.*

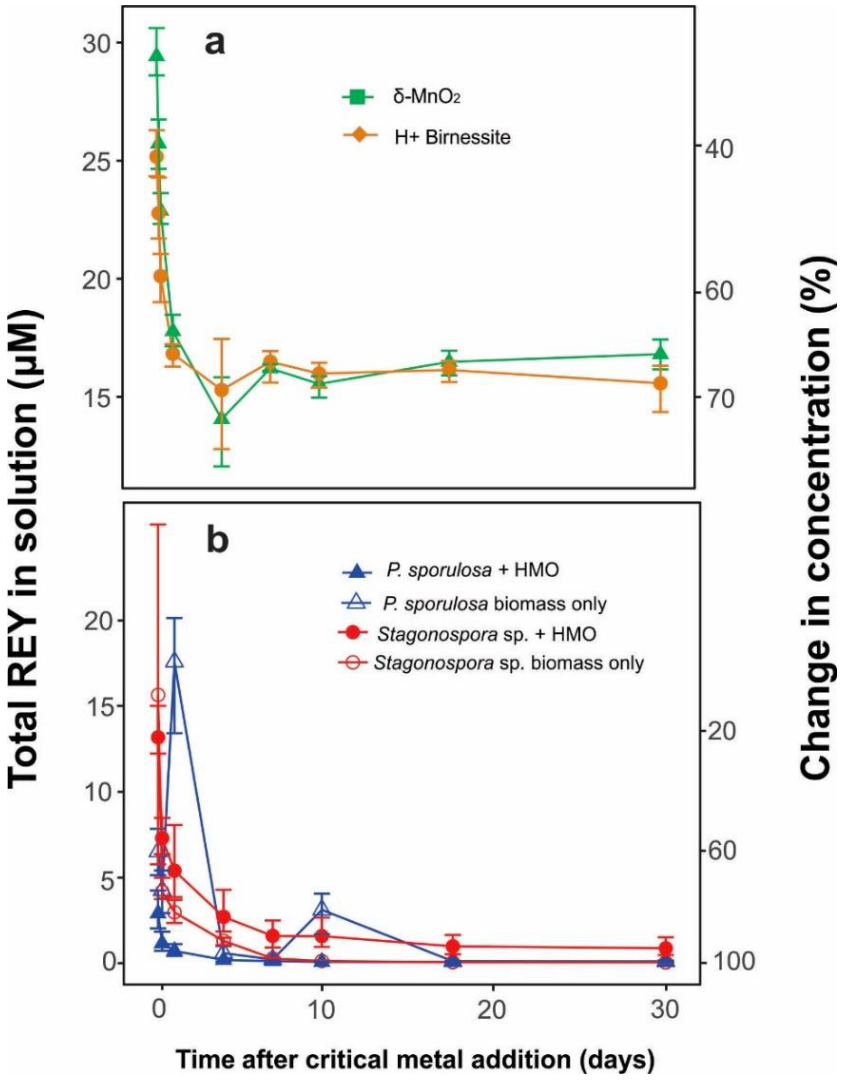

Figure 3. a) Change in total REY concentration in solution in the presence of abiotic δ-MnO_2 and H+ birnessite over the 31-day experiment; **b)** change in total REY in solutions containing fungal biomass with or without HMO. From Boothe-Lordon et al. (in review, 2025).

2.3.2 Hydrous aluminum oxide (HAO) experiments

Modeling of the proposed experimental conditions using PHREEQC indicates that the presence of 10 mM SO_4 results in Al precipitation at a lower pH (4.0-4.5) than in SO_4-free experiments owing to relatively low solubility of basaluminite compared to gibbsite. However, when the SO_4 concentration is increased 3-fold, less Al is precipitated at the same low pH value, presumably due to the formation of aqueous complexes with SO_4 which results in a decreased mass of precipitate. Consequently, for the high-SO_4 scenario, less efficient adsorption of REEs is indicated. Both the availability of sorbent and the potential formation of REE-SO_4-ternary surface complexes explain why REEs are more effectively adsorbed at pH 4.5 in the low-SO_4 solutions compared to the high-SO_4 and SO_4-free solutions.

Two sets of batch experiments involving titration of solutions containing (1) dissolved Al, REE, Sc and Y and (2) synthesized HAO, REE, Sc and Y were conducted with 0, 10 and 30mM sulfate to inform these geochemical models and further elucidate the importance of adsorption and coprecipitation as

mechanisms for REE enrichment in Al-rich phases. The solutions were titrated to a pH of 3-7 in half pH increments. After reaching the desired pH, the solution was allowed to equilibrate for 24 hours and sampled and analyzed.

Figure 4 shows the results of the first experiment in which Al is precipitated with REE. The graph shows the fraction of Al precipitated as pH is increased. In the sulfate-free experiment, the mineral gibbsite is formed and hydrobasaluminite is presumed to be formed in the sulfate experiments. The results show that gibbsite is more soluble at a higher pH than hydrobasaluminite, and hydrobasaluminite is more soluble at pH 4 in the 30mM SO_4 experiment compared to the10mM solution. This difference confirms our hypothesis that higher sulfate concentrations promote the formation of aqueous $AlSO_4$ complexes, which lower the activity of the uncomplexed ion. This study is the first to show the effects of very high SO_4 on Al precipitation.

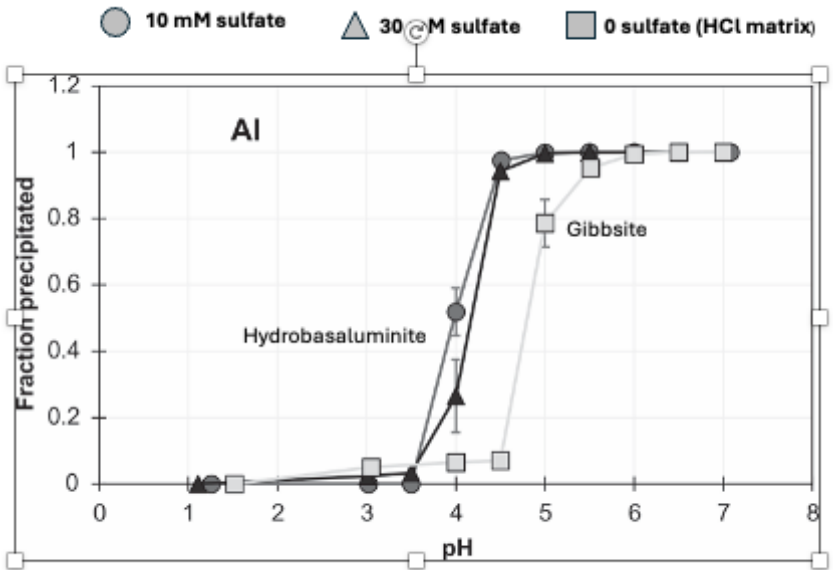

Figure 4. Fraction of Al precipitated as a function of pH in 0-, 10- and 30-mM sulfate solutions.

We also observe that the fraction of REE adsorbed by the Al solids increases at lower pH in the 10mMsulfate solution, although it decreases slightly in the 30 mM sulfate solution (Fig 5.).

The results confirm previous studies that sulfate can increase REE adsorption, but also suggests that at higher sulfate concentrations, REE-sulfate complexation and availability of Al sorbent can reduce REE attenuation. In addition, over the range in which basaluminite precipitates (pH 3.5-4.5), the heavy rare earth elements (HREE, e.g., Lu) are adsorbed at lower pH than light REE (LREE e.g. La), and adsorption of REE does not occur until after Al has begun to precipitate. The transition metal scandium (Sc) however, does coprecipitate with the solids. This data suggests that Al solids such as hydrobasaluminite could be acidified to separate REE in stages. Acidifying to pH 4.5 can recover all of the adsorbed La, 90% of Tb, and 80% of Lu before the HAO begins to dissolve**.**

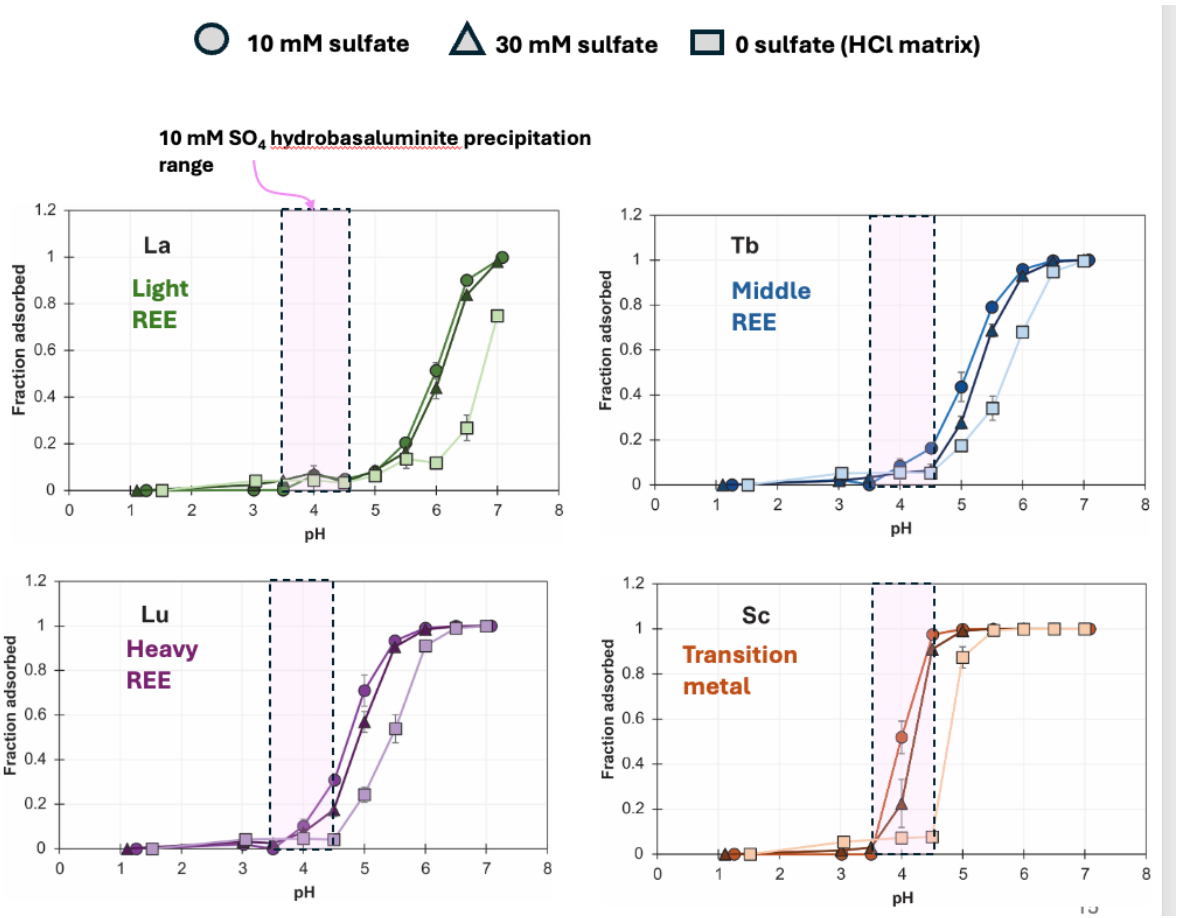

Figure 5. Experiment results showing fraction of REE adsorbed as a function of pH for sulfate-free (square),10 mM sulfate (circle) and 30 mM sulfate (triangle) solutions. The pH range in which basaluminite precipitates is highlighted in purple.

Results of the second set of experiments in which Al is completely precipitated at pH 5-5.5 before REE are added are shown in Figure 6. As in the previous experiment, the REE are adsorbed more readily in the 10 mM sulfate scenario, and there is less adsorption in the no sulfate scenario. However, there is a shift in the adsorption to higher pH when compared to the previous experiment. This is possibly related to less surface area available due to the higher crystallinity of the Al solids precipitated before addition of the REE.

Results of this work were presented by Boothe-Lordon at the 2025 Geological Society of America Northeast and North-central Section Meeting, in Erie, Pennsylvania and as a poster at the Pittsburgh Geological Society Meeting.

2.4 Task 4: Constrain and validate geochemical models

Results from the field observations and bench-scale experiments were used to indicate appropriate default values for adsorption variables and to constraint adjustments of the model parameters within realistic limits. The equilibrium-adsorption model was used to simulate the effects of pH adjustment through specific treatment steps as well as the possible effects of redox state (user input includes dissolved oxygen and concentrations of Fe in 2^+ and 3^+ oxidation states) on the potential for precipitation of pure solids,

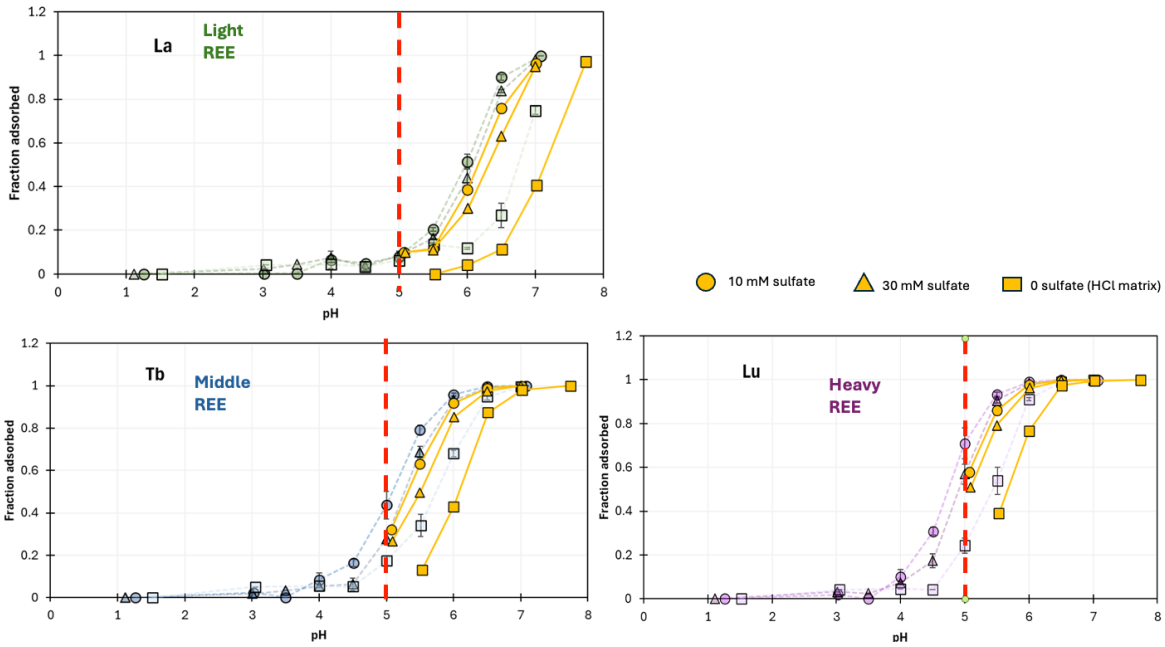

Figure 6. Fraction of REE adsorbed by Al solids as a function of pH are shown in orange (past the dashed red line), superimposed on the results of the previous experiment.

combined with adsorption or co-precipitation of REY. The beta model, modified during Task 1, was further refined to simulate data obtained from experiments conducted as part of Task 3. The initial model was expanded to permit adsorption by both gibbsite and basaluminite as well as potential for co-precipitation (solid solutions) involving Al, La, Ce hydroxides (Figure 7). Surface area of these phases was initially set to a default value of 68 m^2/g, and was subsequently decreased to 32 m^2/g to simulate observations. The calibrated/validated model was then used with the PEST software to compute adsorption equilibrium constants and to identify optimum conditions for the attenuation and recovery of specific REY. The updated adsorption parameters were then used with the kinetics-adsorption model for simulating pH gradients and associated changes in solute concentrations, including oxidation state of Fe and Mn, along the flow path through columns in the laboratory and at one or more field AMD treatment facilities.

Milestones included a) adjusting the modeling database to account for observed precipitation sequences and REY partitioning; b) refinement of models to accurately simulate laboratory and field observations; c) implementation of models to define optimum strategies for REY attenuation and recovery.

2.5 Task 5: Carry out proof-of-concept field test.

The experiments and refined geochemical models will provide a detailed understanding of mineral precipitation reaction sequence and the partitioning of REY as a function of water chemistry changes and interactions with the solids. The experimental observations, including changes in aqueous-phase composition during precipitation, were used to design a proof-of-concept REY capture system deployed in a field setting. The system has been tested at an active, well-characterized AMD site over a period of days to weeks and its performance analyzed by monitoring effluent chemistry and desorbed REY at the conclusion of the experiment(s).

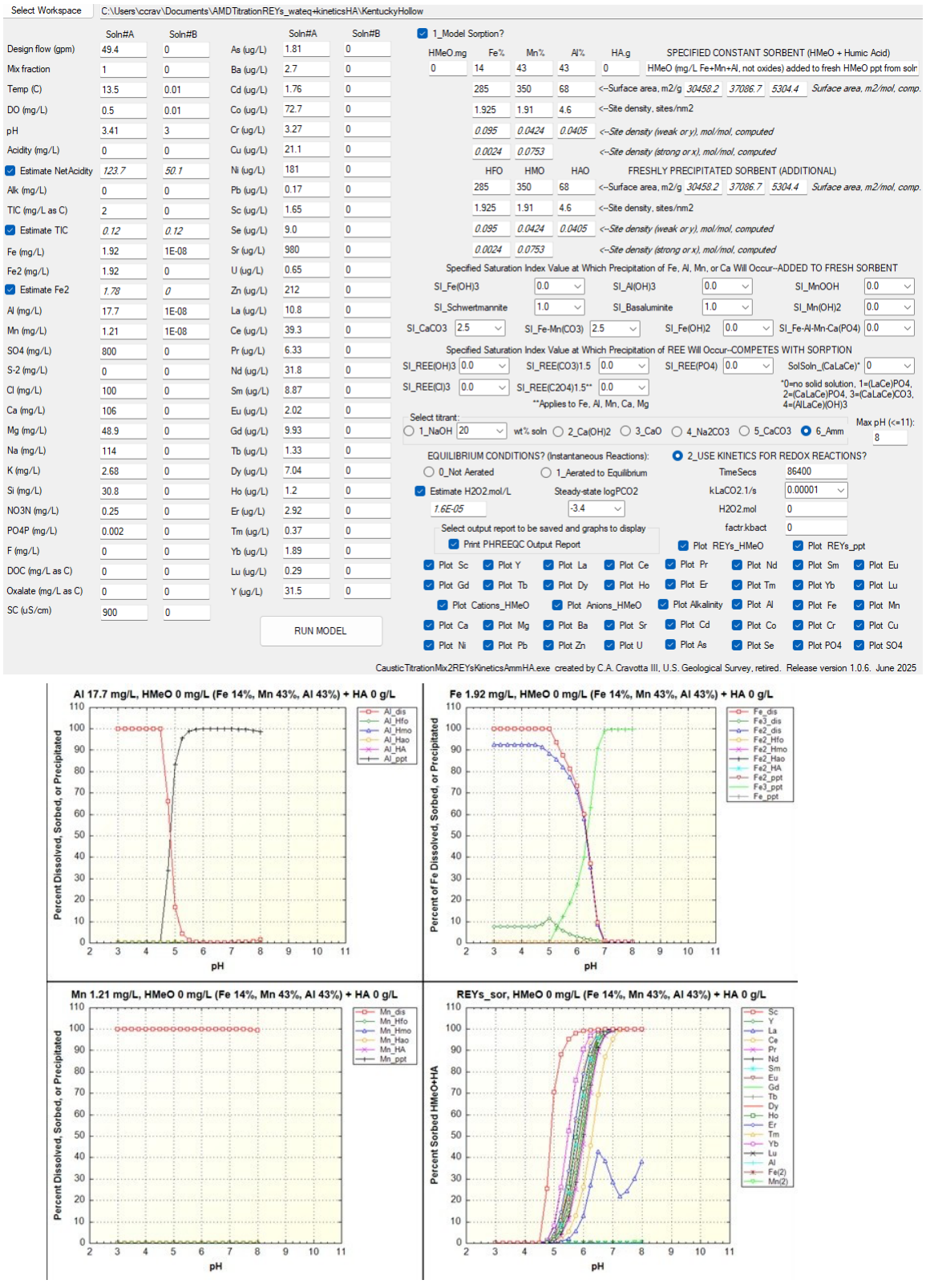

Figure 7. PHREEQ-N-AMDTreat+REYs "CausticTitrationMix2REYsKineticsAmmHA" model, version 1.0.6, showing user-interface with input data for titration of untreated AMD from Kentucky Hollow with ammonium hydroxide and the kinetic simulation results. Thermodynamic data in wateq4fREYsKinetics.dat include constants from Boothe-Lordon et al. (2025).

Milestones included a) design an in-flow system that can be deployed on a scale of weeks under field conditions; b) test the system at an operating AMD treatment site; c) analyze the results of the field tests for follow-on investigations.

The team developed precipitation chambers to understand hydrous metal oxide precipitation and REY adsorption in a field setting. The chambers consisted of a precipitation medium (limestone pellets) encased in a membrane and protected with perforated PVC pipe. To control for the effects of microbial growth, we developed both abiotic chambers (with pore sizes <2 µm to exclude microbes) and chambers that allow microbial infiltration (Fig. 8).

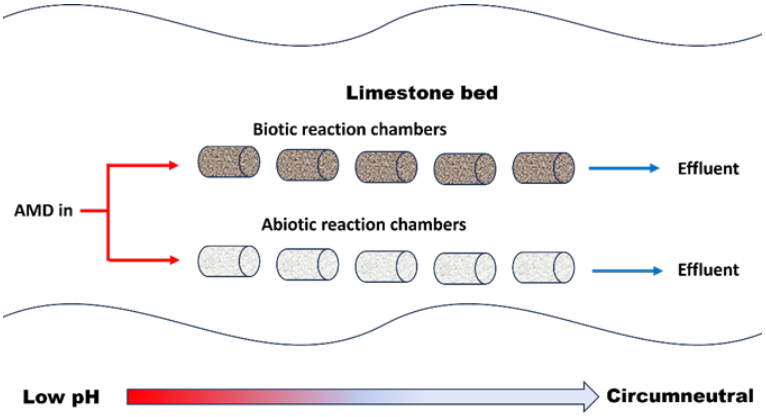

Figure 8. Schematic emplacement of field REE adsorption chambers along a pH gradient.

Prototypes were installed at the Sterrett AMD passive treatment site (Barkeyville, PA) to test initial metal growth and REY adsorption over a period of ~1.5 months. The chambers were emplaced within a limestone treatment bed near the AMD inflow (Fig. 9). The full set of experimental reaction chambers were emplaced at two locations: Kentucky Hollow (high Al) and Sterrett (high Mn). At each location, four replicate sets of chambers were set up, each at a range of three field pH values and each containing multiple substrates.

Figure 9. Emplacement of experimental reaction chambers by Ph.D. student Tashane Boothe-Lordon and co-I Dr. B. Hedin. Left: pH gradient within the Sterrett AMD limestone treatment bed is tested along the flow path. Right: Boothe-Lordon emplaces test precipitation chambers near the AMD inflow.

After the initial 1.5 month test period, apparent growth of hydrous Mn oxides was visually observed in the test chamber emplaced at pH>5, although the amounts were too low to quantify. The apparent growth was greater in the biotic chamber than in the abiotic chamber, indicating that Mn-oxidizing bacteria or fungi played a role. Follow-on work will examine growth of both Mn and Al solids as a function of pH and time, and quantify the adsorption of REY on the solids to allow optimization of REY recovery. Some of this work will be done as part of a separate project supported by NSF.

2.6 Task 6. Estimation of scale-up costs.

Scaling up to a full AMD treatment system with integrated REY capture requires estimation of parameters such as the size/volume of precipitation basins, mixing times required, amounts of additive needed, and the extent to which a passive system can be used in line with the REY extraction.

Cost estimates and value added from REY recovery will be based on the amount recovered, cost of the scaled-up system for REY capture, and the cost for AMD treatment in the absence of REY capture.

Milestones included a) estimated parameters for REY capture from a medium-discharge AMD site; b) estimated cost/return of the REY capture treatment system, in comparison to AMD neutralization and metal removal in the absence of REY recovery.

Calculations for scaling up to field-level REE recovery (Task 5) are pending additional data from reaction chambers.

2.7. Task 7: Technology Transfer

Results of this task included (a) manuscript submission; (b) presentation of results at numerous technical events and (c) national and international research conferences; (d) public availability of modeling parameters; and (e) a final report and written summary fact sheet to OSMRE.

Manuscripts and presentation abstracts are attached in Appendix A.

a. Manuscript submission

Boothe-Lordon, T.J., Capo, R.C., Stewart, B.W., Olds, T. A., Rosenfeld C., 2025, Critical metal removal from simulated acid mine drainage using biotic and abiotic hydrous manganese oxides. Revision under review, *ACS Omega*.

b. Presentation at technical events (*student partially supported by this project)

Boothe* T.J., Rosenfeld C., Stewart B.W., Hedin, B., Capo R.C.(2024) Lab-based assessment of critical metal adsorption by biotic and abiotic hydrous manganese oxides. International Mine Water Assoc. Congress, Morgantown, WV. In: Kleinmann, B., Skousen, J., Wolkersdorfer, Ch.: *West Virginia Mine Drainage Task Force Symposium & 15th International Mine Water Association Congres*s, Morgantown, WV, USA, p. 57-58. https://imwa.info/docs/imwa_2024/IMWA2024_Boothe_57.pdf

Cravotta, C.A. III, Tasker, T.L., Hedin, B.C. (2024) Laboratory and field observations inform geochemical models of treatment strategies to recover rare-earth elements from acid mine drainage. International Mine Water Assoc. Congress, Morgantown, WV. In: Kleinmann, B., Skousen, J.,

Wolkersdorfer, Ch.: *West Virginia Mine Drainage Task Force Symposium & 15th International Mine Water Association Congress*, Morgantown, WV, USA, p. 98–104. https://www.imwa.info/docs/imwa_2024/IMWA2024_CravottaIII_98.pdf.

Stewart, B.W. (2024) Invited virtual presentation: "Rare earth elements in coal mine drainage: Sources and potential sinks." OSMRE Appalachian Region Technology Transfer (ARTT) Critical and Rare Earth Minerals (CREM) Focus Group.

Cravotta, C.A. III. (2025) Invited virtual presentation: "Water-Quality Modeling Tools to Evaluate Potential for Recovery of Critical Minerals from Acid Mine Drainage." OSMRE Appalachian Region Technology Transfer (ARTT) Critical and Rare Earth Minerals (CREM) Focus Group.

Cravotta, C.A. III (2025) Water-quality modeling tools to evaluate potential for recovery of critical minerals from acid mine drainage. *Abandoned Mine Pools as Beneficial Resource Conference*, June 4-5, 2025, Lewisburg, PA. https://www.shamokincreek.org/conference2025

c. Presentation of results at regional/national/international meetings

Boothe T.J., Rosenfeld C., Stewart B.W., Capo R.C. (2023) Experimental investigation of critical metal removal by biotic manganese oxides. *International Goldschmidt Geochemistry Conference, Lyon, France*, Abstract #17181.

Boothe, T.J.*, Capo, R.C., Stewart, B.W. and Rosenfeld, C. (2023) A comparative assessment of critical metal removal by biotic and abiotic hydrous manganese oxides. *Geological Society of America Abstracts with Programs*, v. 55, no. 6, 29-7. https://gsa.confex.com/gsa/2023AM/webprogram/Paper395500.html

Cravotta, C.A. III, Tasker, T.L., and Hedin, B.C. (2023) Empirical observations and geochemical modeling to evaluate treatment strategies for recovery of rare-earth elements from acid mine drainage: *Geological Society of America Abstracts with Programs*, v. 55, no. 6, 213-1. https://gsa.confex.com/gsa/2023AM/meetingapp.cgi/Paper/392405

Boothe, T.J.*, Stewart, B.W., Capo, R.C., and Rosenfeld, C. (2023) Critical element (REE, Co, Ni) sorption by biotic and abiotic hydrous manganese oxides relevant to AMD treatment systems. *American Geophysical Union Annual Meeting*, San Francisco, CA, virtual presentation.

Boothe*, T.J., Capo, R.C., Stewart, B.W., Olds, T. A., Rosenfeld C**. (**2024) Benchtop assessment of critical metal uptake by hydrous manganese oxides under biotic and abiotic conditions. *American Chemical Society Central Regional Meeting*, Pittsburgh, Pennsylvania, Abstract #4166163.

Boothe-Lordon*, T.J., Cravotta C.A., Stewart, B.W., Capo, R.C., Hedin B. C (2025) Effects of sulfate on rare earth element adsorption and coprecipitation by Al hydroxide and hydroxysulfate phases: Batch experiments and equilibrium models. *Geological Society of America Northeast and North-central Section Meeting*, Erie, Pennsylvania, https://gsa.confex.com/gsa/2025NE/webprogram/Paper407795.html

d. Public Access to Data

All data collected over the course of the proposed work are accessible to the public in one or more forms, including (1) through the USGS website or GitHub (*i.e.*, geochemical modeling software release); (2) though peer-reviewed papers, as tables or supplementary information available at the publishers' websites; and/or (3) through electronic data and media submitted to OSMRE as deliverables.

The PHREEQ-N-AMDTreat tool, developed by Co-I Cravotta (Cravotta, 2020; 2021a) was released for public use and will continue to be supported by the USGS. Using information from this study, the REY equilibrium adsorption modeling tool has been refined and validated, and released by USGS as part of the PHREEQ-N-AMDTreat+REYs software (Cravotta, 2021b) for public use.

The PHREEQC and Visual Studio (interface) coding parameters are freely available via the USGS website. The expanded and refined equilibrium adsorption model developed for the project is publicly available and has been incorporated in the publicly available USGS software release product PHREEQ-N-AMDTreat, as a modification to a USGS software release product (PHREEQ-N-AMDTreat+REYs). This includes a new user interface that permits input of humic acid and selection of solid solutions and that will aid the end user in developing more cost-efficient reclamation technologies and provide guidance for efforts to optimize critical REY recovery from AMD.

Data from these studies were also used to develop a strategy for REY extraction at the scale of an individual AMD discharge and have been integrated into the modeling software PHREEQ-N-AMDTreat+REYs (developed by co-investigator Cravotta). This enables the end-user to calculate the cost of different treatment strategies that include REY recovery.

Significance of the Project Results to the OSMRE Applied Science Program

Regardless of shifts in the mining of coal, ongoing AMD discharges will continue to produce massive amounts of solids which will require treatment for the foreseeable future to prevent fouling of waterways. Recovery of rare earth elements from AMD discharges can provide a funding stream for continuing treatment of AMD while supplying a domestic source for critical metal resources. The results of this study can aid in implementation of improved REY recovery systems within AMD remediation systems. By tailoring these systems to preferentially precipitate a REY-rich phase during a specific treatment step, discharges could be treated to meet effluent criteria in combination with recovery of economically valuable REY. Additional revenue from generation of valuable mineral resources provides incentives for AMD treatment for coal operators, community groups and government entities, while addressing national needs.

Because mine drainage outflows vary widely in their chemistry, it is critical to have accurate modeling, that accounts for a range of variables, including discharge chemistry, sorbent properties and processes occurring within remediation systems to allow for the most cost-effective implementation of a resource recovery system, with a minimum of trial-and-error field studies.

The results of this study improve our scientific understanding of important reactions that take place as coal mine drainage interacts with the surface environment and responds to both active and passive treatment methods and addressed key knowledge gaps in our understanding of REY partitioning in solid AMD precipitates and other minerals formed in aqueous environments. Importantly, it provides new parameters for REY affinity and adsorption vs. co-precipitation in solids of different compositions, for which there were few definitive data, including associated pH conditions for optimum REY attenuation.

The combined modeling and lab validation experiments carried out in this study provide important information for active and passive AMD treatment strategies based on metal precipitation and pH-neutralizing reactions. Moreover, data generated from this project can aid in incentivizing treatment of AMD.

Results of this project were presented at three regional technical meetings, two national research conferences and two international conferences (Appendix A).

It also directly contributed to the FOA objective of providing "opportunities for vocational and graduate students to participate in research projects related to coal mining and reclamation issues to build [a] qualified workforce" through funded training and support of a graduate student, leading to a portion of a Ph.D. dissertation on this topic.

Attachments:

Appendix A: PDFs of published abstracts and journal article in review

Appendix B: Written summary fact sheet to OSMRE

References Cited:

Boothe-Lordon, T.J., Capo, R.C., Stewart, B.W., Olds, T.A., Rosenfeld, C.E. (in revision, 2025) Critical metal adsorption by biotic and abiotic hydrous manganese oxides: Implications for acid mine drainage resource recovery. *ACS Omega*.

Cravotta, C.A., III (2008a) Dissolved metals and associated constituents in abandoned coal-mine discharges, Pennsylvania, USA. Part 1: Constituent quantities and correlations. *Appl. Geochem. 23*, 166-202.

Cravotta, C.A., III (2008b) Dissolved metals and associated constituents in abandoned coal-mine discharges, Pennsylvania, USA. Part 2: Geochemical controls on constituent concentrations. *Appl. Geochem. 23*, 203-226.

Cravotta, C.A., III (2020) Interactive PHREEQ-N-AMDTreat water-quality modeling tools to evaluate performance and design of treatment systems for acid mine drainage (software download). *U.S. Geological Survey Software Release (https://doi.org/10.5066/P9QEE3D5)*

Cravotta, C.A., III (2021a) Interactive PHREEQ-N-AMDTreat water-quality modeling tools to evaluate performance and design of treatment systems for acid mine drainage. *Appl. Geochem. 126*, 104845.

Cravotta, C.A., III (2021b) "PHREEQ-N-AMDTreat+REYs" water-quality modeling tools to evaluate strategies for rare-earth element recovery from acid mine drainage. *American Geophysical Union Fall Meeting,* New Orleans, Louisiana, V42A-04.

Cravotta, C.A., III, Brady, K.B.C. (2015) Priority pollutants and associated constituents in untreated and treated discharges from coal mining or processing facilities in Pennsylvania, USA. *Appl. Geochem. 62*, 108-130.

Cravotta, C.A. III, Tasker, T.L., Hedin, B.C. (2024). Laboratory and field observations inform geochemical models of treatment strategies to recover rare-earth elements from acid mine drainage. – In: Kleinmann, B., Skousen, J., Wolkersdorfer, Ch.: West Virginia Mine Drainage Task Force Symposium & 15th International Mine Water Association Congress, Morgantown, WV, USA, p. 98–104. https://www.imwa.info/docs/imwa_2024/IMWA2024_CravottaIII_98.pdf

Hedin, B.C., Capo, R.C., Stewart, B.W., Hedin, R.S., Lopano, C.L., Stuckman, M.Y. (2019) The evaluation of critical rare earth element (REE) enriched treatment solids from coal mine drainage passive treatment systems. *Int. J. Coal Geol. 208*, 54-64.

Hedin, B.C., Hedin, R.S., Capo, R.C., Stewart, B.W. (2020) Critical metal recovery potential of Appalachian acid mine drainage treatment solids. *Int. J. Coal Geol. 231*, 103610.

Hedin, B.C., Stuckman, M.Y., Cravotta, C.A., III, Lopano, C.L., Capo, R.C. (2024) Determination and prediction of micro scale rare earth element geochemical associations in mine drainage treatment wastes. *Chemosphere* 10.1016/j.chemosphere.2023.140475, 140475.

Parkhurst, D.L., Appelo, C.A.J. (2013) Description of input and examples for PHREEQC Version 3—A computer program for speciation, batch-reaction, one-dimensional transport, and inverse geochemical calculations. *U.S. Geol. Surv. Techniques Methods 6-A43*, 497 p.

Stewart, B.W., Capo, R.C., Hedin, B.C., Hedin, R.S. (2017) Rare earth element resources in coal mine drainage and treatment precipitates in the Appalachian Basin, USA. *Int. J. Coal Geol. 169*, 28-39.

Tasker, T.L., Cravotta, C.A. III, and Roman, B. (in review) Sorption of rare-earth elements with hydrous ferric oxide and hydrous aluminum oxide--Roles of sulfate and pH: Applied Geochemistry

Villalobos, M., Toner, B., Bargar, J.R., Sposito, G. (2003) Characterization of the manganese oxide produced by Pseudomonas putida strain MnB1. *Geochim. Cosmochim. Acta 67*, 2649-2662.

Appendix A

- Manuscript submitted to ACS Omega
- Abstracts for technical and scientific meetings

CRITICAL METAL ADSORPTION BY BIOTIC AND ABIOTIC HYDROUS MANGANESE OXIDES: IMPLICATIONS FOR ACID MINE DRAINAGE RESOURCE RECOVERY

Tashane J. Boothe-Lordon[1], Rosemary C. Capo[1], Brian W. Stewart[1], Travis A. Olds[2], Carla E. Rosenfeld[2]

[1] *Department of Geology and Environmental Science, University of Pittsburgh, Pittsburgh, PA 15260*
[2]*Carnegie Museum of Natural History, Pittsburgh, PA 15213*

GRAPHICAL ABSTRACT

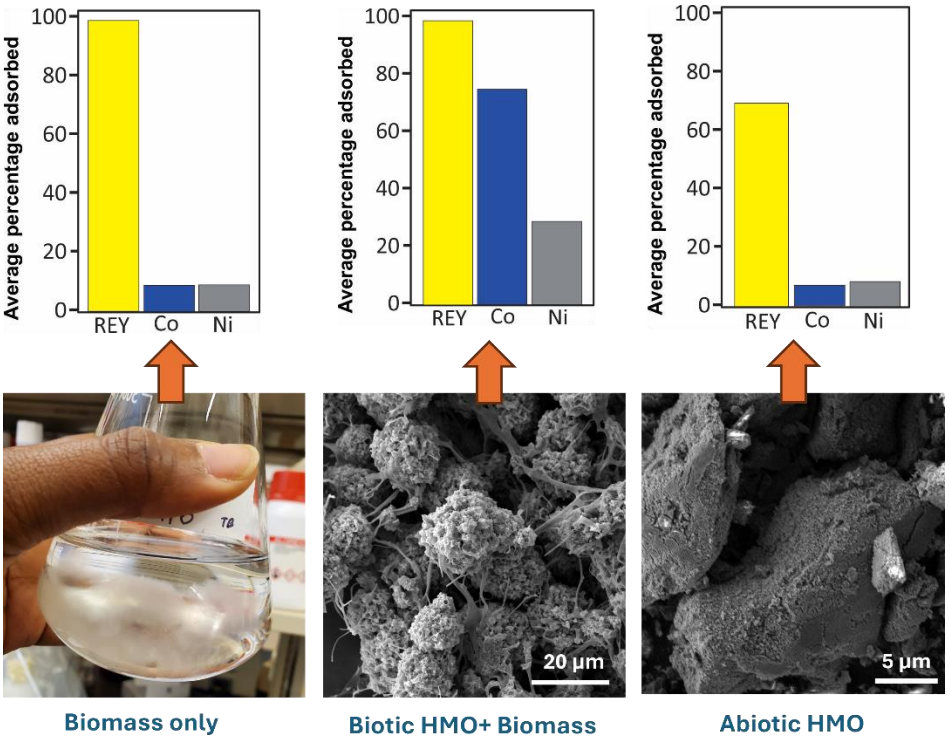

ABSTRACT: Acid mine drainage (AMD) remediation facilities can produce treatment by-products with near ore grade concentrations of rare earth elements (REE), cobalt, and manganese. High concentrations of these critical metals in treatment solids are often associated with hydrous manganese oxides (HMO) through adsorption and/or coprecipitation. Chemical and microbial oxidation processes can influence HMO formation, mineralogy, and sorption efficiency. Here, we investigate the adsorption of rare earth elements and yttrium (REY), cobalt, and nickel over

31 days by (1) HMO (δ-MnO_2 and c-disordered H+ birnessite) produced by chemical oxidation and (2) HMO produced by Mn-oxidizing fungi, *P. sporulosa* and *Stagonospora* sp. Both biotic and abiotic HMO were initially poorly crystalline, but abiotic HMO was transformed to more crystalline phases. After 31 days, ~70% of REY were adsorbed by abiotic HMO, whereas over 99% of REY were adsorbed by biotic HMO and/or fungal biomass within 7 days. Biotic HMO also adsorbed ~30% Ni and ~75% Co; however, Co and Ni adsorption by abiotic HMO was negligible. Abiotic HMO may be susceptible to mineral transformation and dissolution, reducing adsorption capacity. This study shows that biotic HMOs are very efficient at adsorbing certain critical metals and that fungal biomass can also play an important role in this process, especially for REY.

Keywords: REE, cobalt, nickel, fungi, acid mine drainage

Synopsis: Multi-element abiotic and biotic adsorption experiments indicate that hydrous manganese oxides and associated fungal biomass formed in microbially mediated oxidation systems can enhance the recovery of critical metals, such as cobalt and rare earth elements.

1.0 INTRODUCTION

Hydrous manganese oxides (HMO) are common in soils, sediments, and aquatic environments, occurring as crusts, coatings, concretions, and nodules.[1-3] Naturally occurring HMO minerals are typically formed by microbial (e.g., fungal and bacterial) oxidation of Mn(II) to Mn(III) and Mn(IV) via complex catalytic reactions.[4-7] These minerals are generally disordered, poorly crystalline,[8, 9] and highly reactive due to charge imbalances or vacancies in the crystal structures.[2] HMO are environmentally important as they control the aqueous concentration,

transport, and bioavailability of multiple metals, contaminants, and organic compounds through oxidation and adsorption.[2, 10-14] Studies show that these minerals, when synthesized in the lab using known Mn-oxidizing bacteria (e.g., *Leptothrix discophora*, *Bacillus* sp., and *Pseudomonas putida*) or fungi (e.g., *Acremonium* sp., *Pyrenochaeta* sp., and *Plectosphaerella cucumerina*), also have a high capacity to adsorb and coprecipitate metals such as Co, Ni, Pb, Se, and Zn.[15-18] However, chemically synthesized, abiotic analogues of natural HMO minerals can exhibit slower reaction kinetics and reduced efficiency in trace metal uptake when compared to biotic HMO. These differences may stem from variations in chemical and physical properties, such as fewer structural vacancies, altered Mn(III)/Mn(IV) molar ratios, and the absence of organic matter (e.g., biomass or extracellular polymeric substances), which results from differing oxidation mechanisms.[19-22]

The 'metal scavenging' properties of biotic and abiotic HMO have been exploited in many environmental applications including agriculture, drinking water purification, toxic metal remediation, and the recovery of radionuclides.[23, 24] The potential use of HMO in recovering energy-critical metals during acid mine drainage (AMD) treatment has also gained attention due to the high global demand for these metals, the scarcity of ores, and the existing monopoly of supply by few countries.[25-29]

Manganese, as Mn(II), can be a major dissolved species in acid mine drainage (AMD) derived from coal mines. In western Pennsylvania, USA, for example, the average dissolved Mn concentration in AMD (2.35 mg/L) exceeds the Pennsylvania Department of Environmental Protection instream limit of 1.0 mg/L[30], and can be as high as 74 mg/L.[31] Precipitated ochres on the beds of AMD-affected streams in this region can have Mn concentrations over 200 mg/kg,[31] occurring as multiple Mn-oxide and hydroxide mineral phases, including birnessite, pyrolusite,

and todorokite.[3, 10, 32] The Mn content of AMD treatment precipitates typically averages 600 mg/kg and can exceed 400,000 mg/kg in some passive treatment systems.[28, 33] HMO minerals are thought to play a key role in trace metal attenuation (including energy-critical metals such as REY, Ni, and Co) in AMD treatment systems.[28, 32-34] Concentrations of 500-2000 mg/kg REY and greater than 5000 mg/kg Co in some AMD precipitates in Pennsylvania[33] for example, have been attributed to the presence of biotic HMO, particularly in passive treatment systems.[28, 34]

However, not all AMD treatment systems produce precipitates with high critical metal concentrations.[28, 33] In order for AMD treatment solids to become a viable feedstock for critical metals, it is important to not only effectively remove critical metals from solution, but to understand how the biogeochemical conditions in the treatment systems promote their concentration in certain mineral phases. Remaining knowledge gaps include (1) the relative importance of abiotic and biotic HMO in critical metal removal in AMD systems; (2) critical metal attenuation by HMO from multi-element solutions over extended periods (>24 hours), reflecting the complex biogeochemical conditions typical of AMD systems; and (3) comparison of REY and trace metal attenuation by HMO. In most cases, studies on REY behavior tend to focus on synthetic HMO minerals or isolate Ce as the REY of interest.

In this study, we examine the attenuation of ten critical metals[35] (La, Nd, Ce, Gd, Pr, Dy, Yb, Y, Co, and Ni) from solution by HMO produced by two fungal species, *Paraphaeosphaeria sporulosa* (previously *Paraconiothyrium sporulosum*) and *Stagonospora* sp. We also evaluate the importance of fungal biomass in the sorption of these metals. These fungi are known to be present in AMD treatment systems in western Pennsylvania[36] and produce forms of HMO such as vernadite (δ-MnO_2) or birnessite[37] that are highly disordered and have a high adsorption capacity. We also conducted parallel experiments using lab-synthesized δ-MnO_2 and c-

disordered H+ birnessite (hereafter termed H+ birnessite), to examine the interaction of these abiotic minerals with critical metals. The efficiency of critical metal sorption was assessed by conducting time series analyses of the measured dissolved metal concentrations during the experiment. Critical metal recovery is therefore equivalent to its uptake or removal from solution by the HMO substrate. The mineralogy and structure of abiotic and biotic HMO minerals at different time points during the experiments were characterized using scanning electron microscopy (SEM) and X-ray diffraction (XRD) to identify possible mineral transformation and corresponding changes in metal uptake rates. This study expands on previous studies that investigated AMD treatment precipitates using micro-characterization techniques (e.g. by XPS and micro-XRF).[28, 34] Our findings will also inform future field experiments at AMD treatment sites and will also involve the use of these analytical techniques. Our experiments elucidate the role of biotic and abiotic HMO in adsorbing and concentrating various metals in AMD systems, as well as the role of the fungi in this process, with implications for the viability of AMD treatment precipitates as sustainable sources of critical metals.

2.0 MATERIALS AND METHODS

Biotic HMO Experimental Design. Biotic HMO was produced using two common environmental fungal species, *Paraphaeosphaeria sporulosa* and *Stagonospora* sp., originally isolated from a sewage-contaminated pond and an acid mine drainage (AMD) treatment facility, respectively, and maintained in culture at the Carnegie Museum of Natural History in Pittsburgh, Pennsylvania.[37] These fungi are known to be less sensitive to heavy metals and high metal concentrations typical of AMD and are able to tolerate >10 mM of Mn(II).[36] The fungi were

inoculated in triplicate in Erlenmeyer flasks containing 150 ml sterile AY growth media prepared using the method described by Rosenfeld et al.[37] The growth media was buffered at pH 7 using HEPES buffer (0.02 M) and amended with approximately 800 µM $MnCl_2$ to allow the synthesis of HMO by the fungi. Parallel biosorption experiments were also conducted in which both fungal species were inoculated in growth media without the addition of $MnCl_2$ (**Table S1**). All flasks were stored throughout the experiment at room temperature in the dark to limit photochemical reactions. Following inoculation, the fungi were allowed to grow for 14 days, after which the flasks were spiked with critical metal solution containing Co, Ni, Y, La, Ce, Pr, Nd, Gd, Dy, and Yb, dissolved in 10% nitric acid. The concentration of each of the metals in the flasks (**Table S7**) is 70 times higher than the concentration typical of Appalachian AMD.[26] Immediately following the addition of the critical metal solution, the flasks were swirled to mix the solution.

In addition to the fungal HMO and biosorption experiments, two abiotic control experiments (**Table S1**) were also prepared in triplicate to assess critical metal removal in the absence of fungal biomass or biotic HMO. One abiotic control experiment contained growth media and dissolved $MnCl_2$ only, while the second abiotic control experiment contained growth media only without fungi or $MnCl_2$. For each biotic experiment, eight additional flasks were also prepared to allow collection of solid HMO-critical metal precipitates and/or biomass samples at specific timepoints throughout the experiment.

Critical metals and HMO-biomass sampling. Critical metal removal by biotic HMO and fungal biomass was determined by measuring the aqueous metal concentrations at each time point. Aliquots (2 ml) were collected from each flask at 8 time points after the addition of the critical metals: 0.05 h, 6 h, 1 d, 4 d, 7 d, 10 d, 18 d, and 31 d. The lag time between the addition of the solution of critical metals and the retrieval of the first sample (0.05 h) was approximately 2-3

minutes. The samples were filtered using a 0.22 µm mixed cellulose ester (MCE) filter and stored at -20°C. HMO precipitates and biomass were harvested from the additional flasks at the same time points using a vacuum filter with 0.22 µm MCE filters. A sterile plastic spatula was used to dislodge any solids that adhered to the surface of the flask. The filter paper with the solid paste was placed in a small petri dish, sealed with parafilm, and stored at -20°C to prevent desiccation and further oxidation reactions.

Abiotic HMO Experimental Design: The structure and crystallinity of synthetic HMO can vary widely due to structural imperfections, method of synthesis, pH, and aging. [3, 38, 39] Under microbially-mediated conditions in natural and AMD systems, the precipitated hydrous Mn oxide tends to be finer grained, and the structure tends to be less crystalline and more disordered.[15, 40, 41] These structural characteristics, as well as environmental conditions, can result in anomalies in the XRD patterns such as missing peaks, split peaks, and/or broad peaks. The HMO minerals H+ birnessite and δ-MnO_2 are known to be produced naturally by *P. sporulosa* and *Stagonospora* sp.[37] To best approximate the actual HMO substrate produced by these fungi in an AMD treatment system, we used the method of Hinkle et al.[39] to synthesize H+ birnessite and δ-MnO_2.

The experimental conditions of the biotic experiments described above were replicated by suspending approximately 9.2 mg of H+ birnessite and δ-MnO_2 in 150 mL of sterile AY growth media, buffered at pH 7. The solutions were equilibrated for one hour before adding critical metal solution. Each experiment assessing dissolved metal concentrations was conducted in triplicate and proceeded for 31 days at room temperature in a dark environment with nine additional flasks from which solid-phase abiotic HMO-critical metal precipitates were harvested. Sampling of the critical metal-growth media solution and abiotic HMO solids was conducted in a

similar manner to the biotic experiments at nine time points after the addition of the critical metals: 0.05 h, 3 h, 6 h, 1 d, 4 d, 7 d, 10 d, 18 d, and 31 d. Samples were also stored in a similar manner to the biotic experiments.

Analytical techniques. Filtered solution samples (2 mL) collected from all flasks were acid-digested using 300 µL of concentrated trace-grade nitric acid in trace metal-free centrifuge tubes. Samples were allowed to react with the concentrated HNO_3 for 2 hours at 60°C before diluting with distilled-deionized water (dd-H_2O) to 10 mL (final HNO_3 concentration of 3%). Samples were analyzed using a Thermo iCAP Q inductively coupled plasma mass spectrometer (ICP-MS) at the Northwestern University Quantitative Bio-element Imaging Center (QBIC). Blank samples containing 3% nitric acid and dd-H_2O only were also analyzed for quality control. The method of correcting the adsorption data is detailed in the **Supplementary Information**.

Powder X-ray diffraction (PXRD) and scanning electron microscopy (SEM) analyses were conducted at the Carnegie Museum of Natural History, Pittsburgh. PXRD data for air-dried biotic and abiotic HMO samples were obtained using a Bruker Apex II Single-Crystal X-ray Diffractometer (SCXRD) equipped with air-cooled Mo*K*α (λ = 0.71075 Å)/50 kV, 40 mA) IµS 2.0 microfocus source and Photon III CPAD detector. Identifications were made using the PDF 5+ International Centre for Diffraction Data (ICDD) database, paired with Materials Data (MDI) Jade Pro software. A pseudo Gandolfi-like motion was used to randomize diffraction from each sample, which had an average volume of ~$2x10^{-3}$ mm^3. The observed *d*-values and intensities were derived by full-profile fitting using JADE Pro. SEM imaging was done on a Tescan Vega II XMU variable pressure instrument with Oxford Instruments INCA Energy 250XT Energy Dispersive X-ray Analysis system. Air-dried biotic samples were gold coated using a Denton Vacuum Desk V Sample Preparation system.

3.0 RESULTS AND DISCUSSION

Abiotic and Biotic HMO Products. The abiotically synthesized HMOs, δ-MnO_2 and H^+ birnessite, have layered, angular structures (Fig. S1) and likely have cation vacancies and/or high Mn(III) content.[18, 38] PXRD patterns of δ-MnO_2 and H^+ birnessite prior to the experiments show broad symmetrical peaks at 29.3° 2θ and 17° 2θ corresponding to the (310)/(020) and (200)/(110) planes. There is also a broadening and apparent splitting of the peaks at ~7.6° 2θ (Fig. 1a). For H+ birnessite, the characteristic 002 reflection expected at 11.3° 2θ,[2, 42] is absent. Additionally, for δ-MnO_2, the basal peak at 5.5° 2θ forms a shoulder, but this is absent in the H^+ birnessite pattern. These shifts and irregularities in the basal reflections (00*l*) of the abiotic HMOs relative to other reported XRD (e.g. Drits et al.[43]) have also been reported in previous studies,[40] underscoring the high levels of disorder in the sheet stacking arrangement and variations in interlayer compositions typical of phyllomanganates.

After 31 days, both abiotic HMOs underwent phase transformation. δ-MnO_2 appears to have been transformed into a multi-phase solid that is not readily identifiable. H^+ birnessite was also transformed to ramsdellite as shown by the major peak positions at 24.8° 2θ, 19° 2θ, 16.7° 2θ, and 10.15° 2θ (Fig.1a). Ramsdellite is a tunnel structure Mn-oxide formed by linking adjacent single chains to form double chains[44] and is composed of Mn(IV).[45] Aging, as well as the interaction with other cations, can transform layered HMO to more crystalline tunnel varieties.[13, 37, 46] Given the increase in Mn(II) in solution (Fig. S6), we hypothesize that a partial reduction of Mn(IV) in H+ birnessite by Ce, Co and/or interaction with the HEPES buffer resulted in the formation of Mn(III) which subsequently underwent disproportionation to produce Mn(IV) and aqueous Mn(II).

The biotic HMOs produced by *Stagonospora* sp. and *P. sporulosa* in these experiments are poorly crystalline; however, unlike the abiotic HMO, they remained relatively stable over the duration of the experiment. Both fungi produced an amorphous solid or a poorly crystalline phyllomanganate resembling vernadite (or its synthetic analogue, δ-MnO_2) with very weak peaks at 29.3 2θ and 17° 2θ (Fig. 1b). Aging and cation interaction did not result in significant mineral transformations. After 31 days, the biotic HMO products showed stronger peaks at 29.3 2θ and 17° 2θ corresponding to the in layer (310)/(020) and (200)/(110) planes, respectively. δ-MnO_2 is produced by both bacteria and fungi in the presence of Mn(II).[13, 37, 46, 47] Crystals of this mineral phase occur as exceptionally thin sheets, typically less than 100 nm in length. These sheets exhibit strong disorder, manifested as random stacking sequences of Mn–O sheets and variably populated interlayer cation and H_2O content, resulting in weak, broad, or absent (001) and (002) reflections.[2] For all samples studied here, the (001) basal peak at 5.4° 2θ is largely absent, confirming the presence of small crystals and high levels of disorder. The broad peak at 7.8° 2θ is possibly due to the presence of chitin in the fungal cell wall.[37, 46] These XRD patterns suggest that the fungal δ-MnO_2 remained stable and highly reactive throughout the experiment and may explain the high sorption capacity of the biotic HMO.

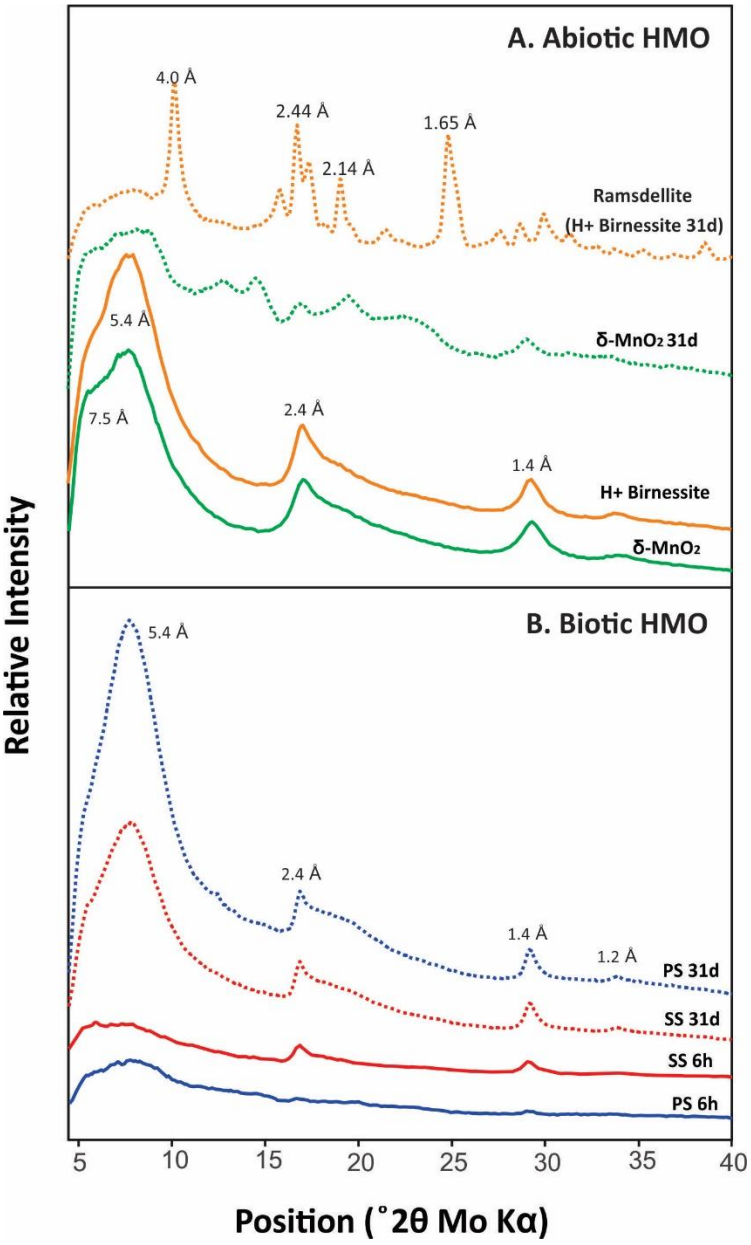

Figure 1a. X-ray diffraction (XRD) pattern of abiotic HMO δ-MnO_2 and H+ birnessite before critical metal addition and 31 days after critical metal addition (δ-MnO_2 31d and H+ birnessite 31d) metals. **Figure 1b.** XRD patterns of biotic HMO produced by *P. sporulosa* retrieved after at 6 hours (PS 6h) and 31 days (PS 31d) and *Stagonospora* sp. retrieved at 6 hours (SS 6h) and 31 days (SS 31d).

While outside the scope of this project, other structural characteristics such as surface area measurements of the biotic and abiotic HMOs could offer additional points of comparison. Although the surface area of HMO minerals can be variable depending on the synthesis method,[23] biotic HMOs tend to have a larger surface area than abiotic HMO.[15, 48] However, surface area is not expected to be a limiting factor for critical metal adsorption in these experiments, given the concentration of Mn used in our experiments (~800uM), and reported surface area and site density of biotic and abiotic HMO.[49] Nevertheless, the behavior of the biotic and abiotic HMO minerals during these experiments could be constrained in future work by using controls such as abiotic oxides aged in media without critical metal additions, abiotic HMO amended with Mn(II), or abiotic HMO incubated with biomass. Similarly, the use of alternative growth media with lower organic carbon content could help eliminate potential interactions between organic molecules and dissolved metals.

The HMO precipitates that formed through fungal oxidation were associated with the fungal biomass, either directly on the hyphae or in the interstitial (extracellular) areas (Fig. 2). HMO precipitated by *P. sporulosa* encrusts the entire length of the hyphae (Fig. 2a-b) and is similar to the morphology of HMO produced by the fungus *P. cucumerina*.[50] Unlike *P. sporulosa*, HMO produced by *Stagonospora* sp. occurs as larger, spherical structures (approximately 30 μm) adjacent to the fungal hyphae. The HMO produced by both fungi consists of an aggregation of randomly oriented plate-like structures with erose edges, similar to those described in previous studies.[48, 50-52] This gives the biotic HMO a sponge-like or crumpled appearance very dissimilar to the blocky, angular grains of the abiotic HMOs (Fig. S1).

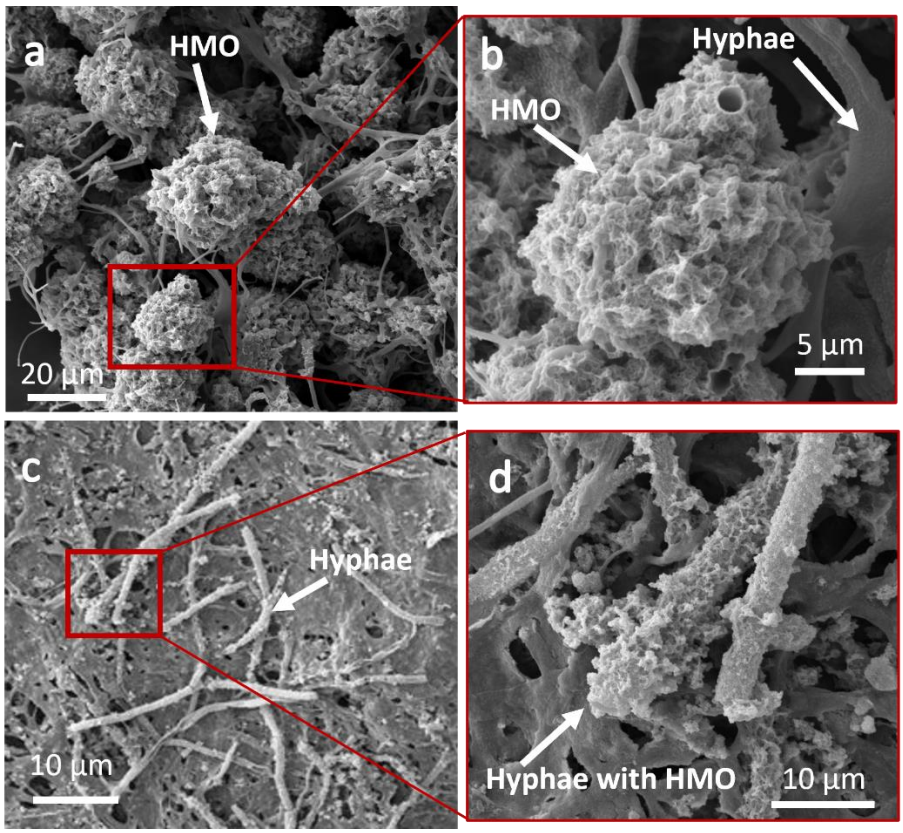

Figure 2 a-b. Scanning electron microscopy (SEM) images of *Stagonospora* sp. biomass retrieved at 31 days showing the occurrence and associations of HMO minerals. **Figure c-d**. SEM images of *P. sporulosa* retrieved at 31 days showing the occurrence and associations of HMO minerals.

Previous studies have shown that *Stagonospora* sp. and *P. sporulosa* produce HMO with Mn(III) and Mn(IV) content varying from 80% - 97%. [37, 50, 53, 54] Fungi oxidize Mn(II) via hyphae-associated superoxide production,[55] by the production of cell-wall associated enzymes such as multicopper oxidase,[51] and by cell-free secretomes (biomolecules) mediated by extracellular proteins.[56] While it is unclear whether these processes occur concurrently, the precipitation of hyphal-associated HMO (as in the case of *P. sporulosa*) suggests that superoxide production and cell wall enzymes may be the dominant mechanisms for Mn(II) oxidation. Oxidation of Mn(II) by extracellular proteins could explain the location of HMO in interstitial area of the biomass as seen with *Stagonospora* sp. This difference in the morphology and

location of the biotic HMO has been cited as evidence that the mechanism for fungal Mn oxidation can vary among species.[57]

Stagonospora sp. and *P. sporulosa* showed a marked difference in the amount of dissolved Mn oxidized to form HMO. Over the 14-day growth period, *Stagonospora* sp. oxidized approximately 30% more dissolved Mn than *P. sporulosa* (Fig. S2). This variation in Mn oxidation capacity may be attributed to differences in growth rates, metabolic processes, or oxidation mechanisms involving reactive oxygen species, proteins, and enzymes.[51, 55, 56] The effects of growth rate on Mn oxidation could be assessed by normalizing HMO production to biomass produced. However, because the biotic HMO are strongly bound by, and enmeshed in, the fungal biomass, we were not able to directly measure the fungal biomass.

Throughout the experiments, dissolved Mn content fluctuated as a response to interactions of HMO with metals (Fig. S2). Following the addition of critical metals, dissolved Mn concentrations increased from almost undetectable (2.5 µM) to 60 µM in the *Stagonospora* sp. experiment over 31 days. Conversely, in the *P. sporulosa* experiment, dissolved Mn concentrations declined after the addition of critical metals, from 270 to 180 µM representing an additional 11% decrease in dissolved Mn over 31 days. These changes in aqueous Mn(II) concentrations reflect the complex redox reactions occurring between previously formed HMO and the critical metals, particularly Co(II) and Ce(III). Co(II) and Ce(III) are readily oxidized by Mn(IV), [15, 16, 25, 46, 58] producing Mn(II) through the disproportionation of Mn(III) ions.[41, 42] Continuous, slow decline in Mn(II) concentrations in the *P. sporulosa* experiment suggests that the presence of the critical metals may have slowed but not completely inhibited Mn(II) adsorption and/or oxidation.

Adsorption of transition metals Co and Ni by HMO. The abiotic HMOs used in our experiments were relatively inefficient at sorbing Co and Ni. Initially, there was a steady decline in Co and Ni concentrations in both the δ-MnO_2 and H+ birnessite experiments, with maximum adsorption of these metals occurring on day 4 (29% and 19% Co adsorbed, respectively, and 24% and 18% Ni adsorbed, respectively (**Fig. 3a, b**)). Subsequently, Co and Ni concentrations in both experiments increased due to desorption. Overall, the adsorption of Co and Ni in these experiments was minimal over 31 days, with δ-MnO_2 adsorbing 4.5% of the metals, while H+ birnessite removed approximately 11% of the metals.

The low adsorption of Co and Ni by the abiotic HMO may be due to the transformation of δ-MnO_2 and H+ birnessite into secondary or tunnel crystalline HMO phases. Tunnel structure HMO minerals, such as ramsdellite, are highly crystalline and have been reported to exhibit very low Co and Ni absorption in multi-metallic solutions.[16, 41] In contrast, synthetic H+ birnessite and δ-MnO_2, which possess a layered or sheet-like structure, readily adsorb Co and Ni in mono-metallic solutions.[15, 17, 59] In multi-metal solution, however, these synthetic layer type HMO adsorbs significantly less metals.[17, 59, 60] This highlights not only the importance of the type of HMO phases but also the influence of competing metal ions on adsorption efficiency.

Biotic HMO produced by *Stagonospora* sp. and *P. sporulosa* are very efficient at adsorbing Co (**Fig. 3c**). Dissolved Co concentrations declined rapidly and steadily in the *Stagonospora* sp. experiment, resulting in greater than 80% of Co adsorbed over 31 days. In the *P. sporulosa*- HMO experiment, Co concentrations decreased less rapidly in the first 6 hours. Desorption and subsequent fluctuation in Co concentrations in the first day of the experiment resulted in 12% less Co adsorbed than *Stagonospora* sp.- HMO.

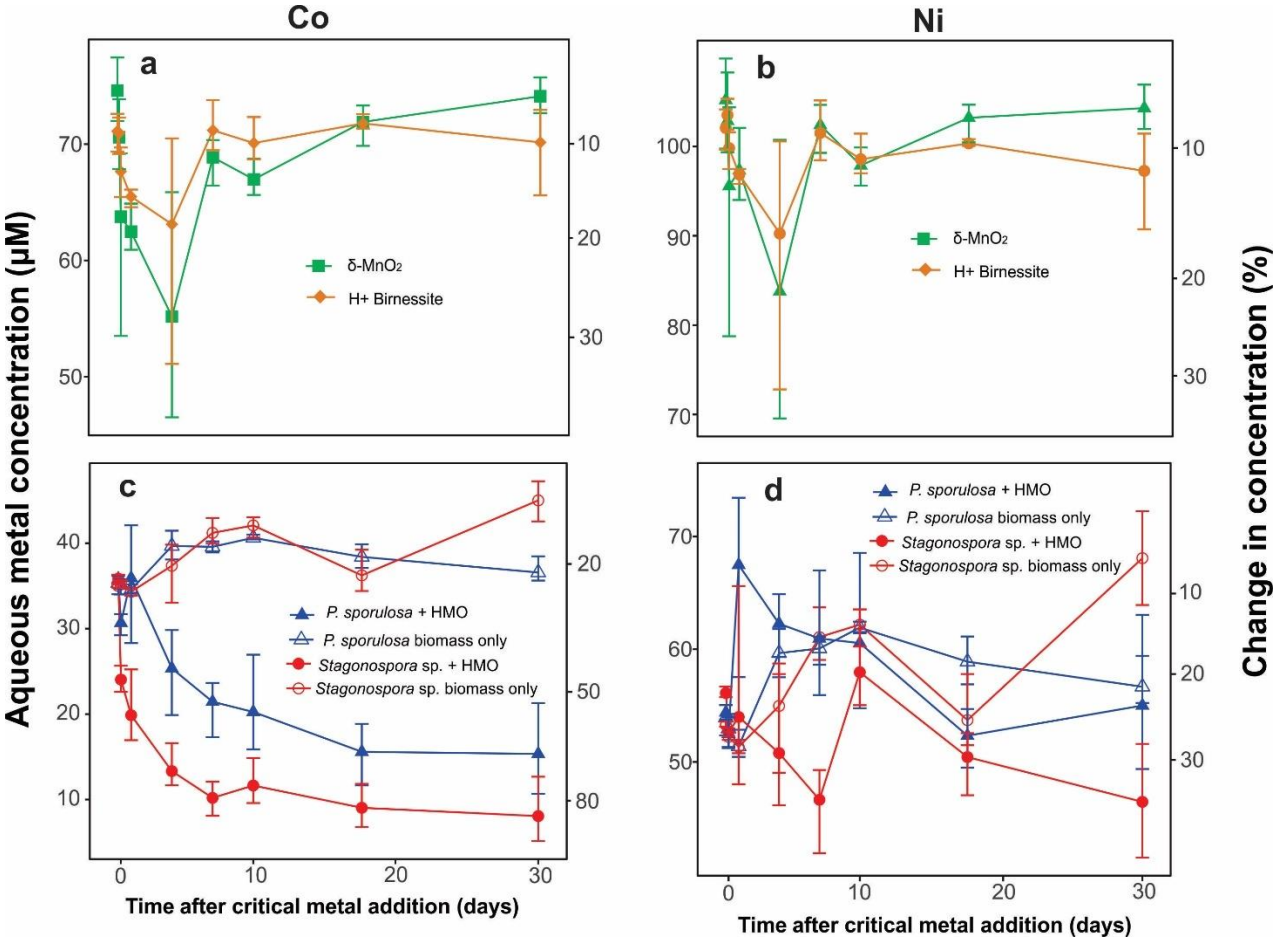

Figure 3. Change in dissolved Co and Ni concentrations in the presence of: **a-b.** Abiotic HMO, δ-MnO_2 and H+ birnessite; **c-d**. Biotic HMO produced by *Stagonospora* sp. and *P. sporulosa* and/or *Stagonospora* sp. and *P. sporulosa* biomass. Each point presents the average value for three replicate experiments. The top and bottom of the error bar represent the maximum and minimum values respectively.

HMO is known to readily adsorb Co due to strong redox reactions with Co(II).[17, 41, 61] Up to 80-90% of Co adsorbed on HMO can be present as Co(III) or Co(IV).[10, 15, 46] The poorly crystalline, vacancy-rich biotic HMO products of *Stagonospora* sp. and *P. sporulosa* are likely responsible for the rapid adsorption of Co observed in these experiments, as Co(III) is typically incorporated into layer vacancies in the HMO structure [17, 41, 52] or at corner- and edge-sharing sites.[41, 46] Importantly, studies also show that Co will fill edge sites preferentially before

diffusing to layer vacancies.[61] This has implications for other trace metals such as Ni that are also adsorbed at the edge sites or incorporated into HMO structure.

Over 31 days, HMO produced by *Stagonospora* sp. adsorbed 12% more Ni than HMO-*P. sporulosa* (Fig. 3d). However, for both biotic HMO experiments, the amount of Ni adsorbed after 31 days was not significantly different from values recorded within the first day of the experiment. This is because Ni concentrations fluctuated widely, particularly between day 1 and day 10, reflecting considerable amounts of desorption. Less Ni was adsorbed by biotic HMO (3.15 µmole) compared to Co (5.55 µmole), even though the concentration of Ni was 1.5 times greater than Co in the spiking solution. This is consistent with previous studies that also show preferential adsorption of Co over Ni. [16, 41, 49] While Ni may be incorporated into layer vacancies,[18, 62] most studies report that Ni is located near layer vacancies to form corner-sharing Ni(II) species in the HMO structure or at edge sites.[18, 41, 59, 63] However, as discussed previously, Co will fill edge sites preferentially before diffusing to layer vacancies[61] and Ni does not compete with Co for these edge sites. [41] Thus, the presence of Co can result in three times lower adsorption of Ni onto HMO.[16]

Because the biotic HMO is associated with the fungal biomass, there is potential that the biomass contributes to the adsorption of Co and Ni. However, this study did not identify significant biosorption of Co or Ni in the biomass-only experiments (**Fig. 3c-d**). *P. sporulosa* biomass removed approximately 20 % of Co and Ni whereas *Stagonospora* sp. biomass removed less than 10% of these metals. This indicates that biomass alone does not contribute significantly to adsorption in these experiments and underscores the importance of biotic HMO in controlling metal adsorption, particularly Co. The lower uptake of Co and Ni by the biomass, compared to the biotic HMO, may be attributed to differences in surface area and the quantity and types of

sorption sites. Previous studies show mixed results on Co and Ni biosorption, with some reporting minimal adsorption by fungal biomass [41, 46, 48] and others reporting significant Co and Ni biosorption by fungal [64-66] and bacterial biomass.[67, 68] This suggests that the sorption capacity can vary significantly among microbial species, experimental conditions, and possibly the availability of binding sites in multi-metallic or mono-metallic solutions.

Adsorption of REY by HMO. In all experiments, the REYs exhibited higher adsorption rates compared to Co and Ni in the same experiment. The abiotic HMOs adsorbed approximately 70 -73% of the REYs by day 4 of the experiment. Like Co and Ni, desorption of adsorbed REY was observed on day 4 (**Fig. 4a**), likely due to the phase changes in the abiotic HMO. However, in this case, REY desorption was minimal, with 68–71% of the REY remaining adsorbed after 31 days.

In contrast, all REYs were rapidly adsorbed in the biotic systems (**Fig. 4b**). HMO-*P. sporulosa* was more efficient than HMO-*Stagonospora* sp., with greater than 90% of total REY adsorbed within 6 hours. HMO-*Stagonospora* sp. adsorbed 90% of total REY within 7 days. Overall, the REYs are more readily adsorbed than Co and Ni, with over 99- 99.9% adsorption over 31 days. Interestingly, HMO-*Stagonospora* sp., which was the most efficient at adsorbing Co and Ni, adsorbed less REY than HMO-*P. sporulosa*.

The high adsorption efficiency of REYs observed in these experiments (>99 %) is typical of AMD treatment systems which generally have efficiencies exceeding 90%.[34] This highlights the importance of HMO phases in treatment solids for REY adsorption. However, given the high REY adsorption observed in the biomass-only experiments (discussed below), it is likely that REY adsorption by the biotic HMO in these experiments includes a contribution from the biomass.

Substantial amounts of REYs were removed through biosorption, in contrast to our observation for Ni and Co. REY concentrations decreased rapidly in the presence of *P. sporulosa* and *Stagonospora* sp. biomass at rate similar to or greater than those observed in the biotic HMO experiments (**Fig. 4b**), demonstrating that fungal biomass can serve as an effective sorbent for REYs.

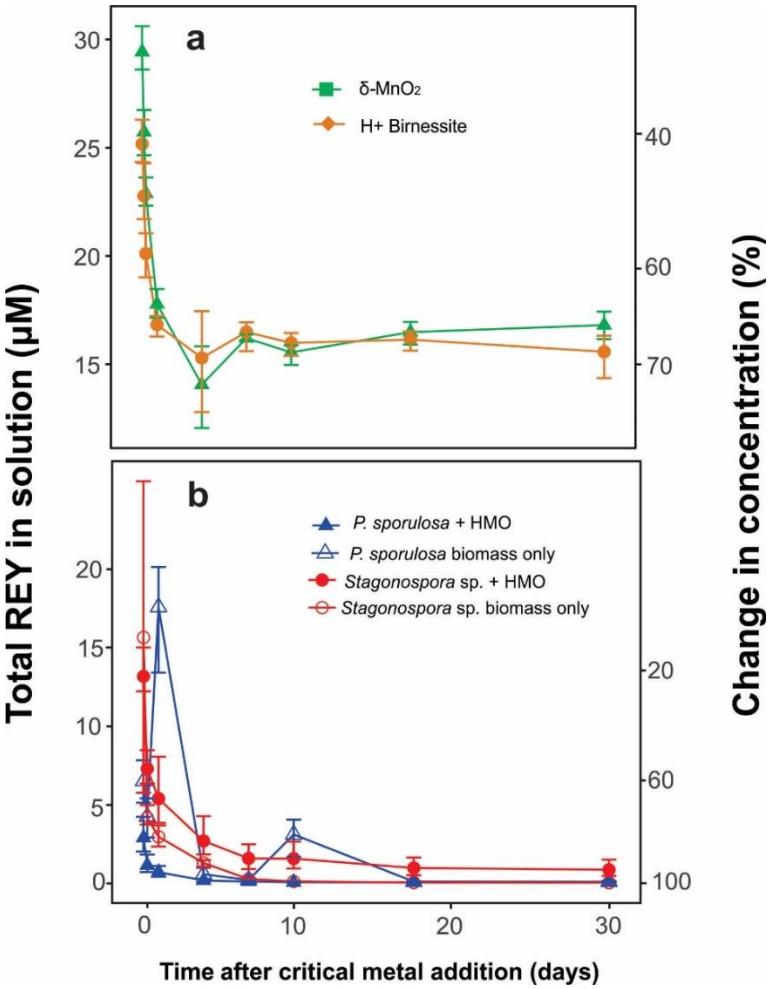

Figure 4. Change in dissolved Co, Ni and total rare earth element (TREE) concentrations in the presence of (**a**) abiotic HMO and (**b**) biotic HMO and/or fungal biomass after the addition of critical metals. Each point presents the average value for three replicate experiments. The top and bottom of the error bar represent the maximum and minimum values respectively.

The process of biosorption does not typically result in oxidation of adsorbed metals. For example, redox-sensitive metals such as Ce and Co associated with bacterial and fungal cells remain in their +3 and +2 states, respectively, suggesting that biosorption inhibits oxidation. [15, 25, 64, 69] Instead of oxidation, biosorption occurs through ion exchange, complexation, or electrostatic interactions between metal ions and functional groups on the cell wall.[70, 71] These functional groups originate from chitin, and other polysaccharides and glycoproteins such as glucans and mannans in the fungal cell wall.[70, 72] The specific functional groups involved in biosorption for an individual species are difficult to ascertain, especially for fungi;[72] however, certain groups are known to play a key role. For instance, carboxyl and phosphate functional groups are known to facilitate Eu(II) adsorption by bacteria[73] and sulfhydryl sites have been shown to be the dominant adsorption sites for some divalent ions at environmentally significant concentrations.[74]

The biotic HMO, biomass-only, and abiotic HMO systems display preferential adsorption of light rare earth elements (LREE) compared to the middle rare earth elements (MREE) or heavy rare earth elements (HREE) (**Fig. 5**). This difference is more pronounced in the *Stagonospora* sp.- HMO and *Stagonospora* sp. biomass experiments after 31 days (Fig. 6), with roughly one order of magnitude more LREE adsorbed than HREE. Preferential adsorption of LREE by HMO has previously been observed experimentally,[58] in natural AMD precipitates,[34] and in groundwater systems.[75] The fungal species involved in the experiment also appears to influence the REE patterns. The experiments involving *Stagonospora* sp. display very similar concave LREE pattern, whereas the *P. sporulosa* experiments display a relatively flat LREE pattern.

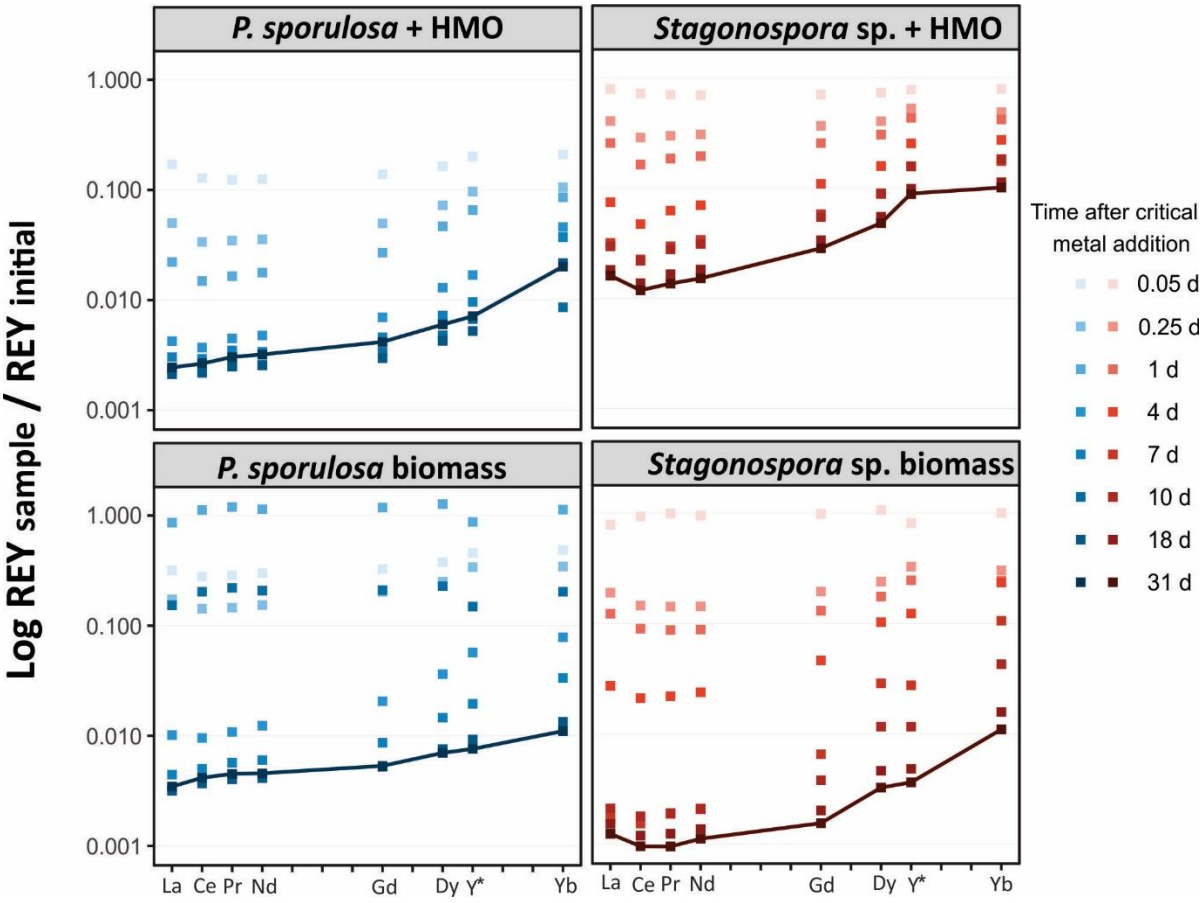

Figure 5. Ratio of REY in solution at each sample point to the initial concentration in the flask. Yttrium is plotted in the position of Ho (not analyzed) due to its nearly identical ionic (3+) radius. Biotic HMO with biomass, and fungal biomass only removed greater than 99% after 6 hours and greater than 99.9% after 7 days. Each point presents the average value for three replicate experiments.

Despite the preferential adsorption of the LREE, we note an apparent lack of Ce anomalies in all experiments (Fig. 6). Cerium is readily oxidized by HMO, which could lead to preferential Ce incorporation in the HMO mineral. This process reduces the concentration of Ce in the solution relative to its neighboring REYs, creating a negative Ce anomaly (low normalized Ce concentration relative to other REYs). [25, 58] Weak or absent Ce anomalies for all experimental conditions may imply that significant Ce(III) oxidation did not occur. However, it is possible that the anomaly was erased by the rapid uptake of all the LREE at pH 7.[76] Cerium anomalies may be more likely in acidic solutions because at these conditions, other trivalent REY ions are inhibited

from being adsorbed onto HMO.[69, 77] Experiments have also shown that REYs are preferentially complexed by organic compounds before being adsorbed to HMO, which can also prevent Ce anomalies from developing. [76, 78]

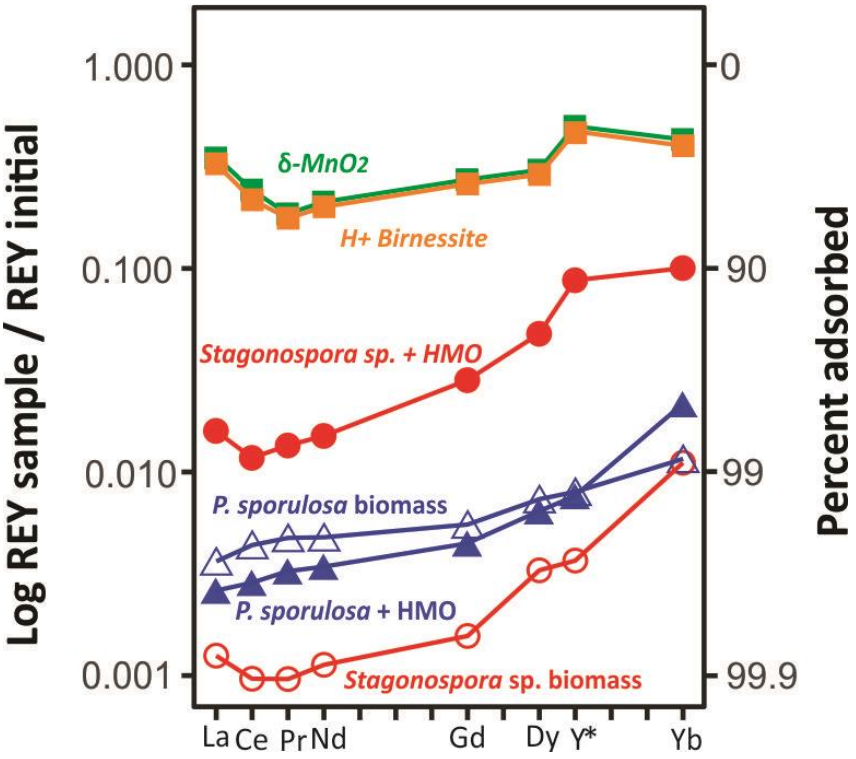

Figure 6. Comparison of the REY patterns after 31 days. Ratio of REY in solution at each sample point to the initial concentration in the flask.

4.0 ENVIRONMENTAL IMPLICATIONS

HMO in AMD treatment solids is disproportionately enriched with REY relative to other common metal oxides, such as hydrous Fe and Al oxides.[33, 34] Manganese in AMD can be difficult to treat and is best removed at pH >9 using strong oxidants.[30, 79] However, in passive AMD treatment systems that rely on natural chemical and microbial processes, microbes, including the fungi explored in this study, mediate the precipitation of HMO at around pH 7.[36, 80]

Our experiments demonstrate that at this pH, the biotic HMO rapidly adsorbs 70-99.9% of Co and REY but only 30% of Ni. Both biotic and abiotic HMO are poorly crystalline; however, biotic HMOs exhibited greater stability and resistance to structural changes over time when compared to abiotic analogues formed through chemical oxidation. The stability of the biotic HMO may be related to ongoing Mn redox cycling facilitated by the fungi, which helps to maintain the highly reactive nature of biotic HMO over time. In contrast, the abiotic HMOs undergo phase changes accompanied by desorption over time, resulting in considerably less critical metal adsorption.

Microbes in AMD treatment systems (including fungi and bacteria) may be associated with mineral surfaces or other suspended organic solids.[81] Microbial biomass associated with HMO minerals may provide an additional surface on which adsorption can occur since studies show that biomass does not compete with or prevent adsorption of trace metals by HMO.[82, 83] Our study shows that fungi have varying biosorption capacities or affinities for different metals. This alludes to potential competition or preference by these metals for functional groups on the cell wall of the fungi. Fungal biomass, in this study, rapidly adsorbed 90-99.9% of REY, indicating a strong affinity for these elements. Because fungal biomass appears to preferentially accumulate REY over Co and Ni, there is potential for exploiting biosorption as a mechanism for selective REY recovery. However, the long-term fate of critical metals adsorbed to biomass remains unclear. Some studies have shown desorption of REY [25, 84] and the dissociation of REY-organic ligands bonds over time,[78] potentially allowing these metals to become adsorbed and/or oxidized by hydrous metal oxides. REY adsorbed to biomass on surfaces may eventually become incorporated within HMO structure and other oxides after death of the fungi and decomposition of the biomass. In contrast, critical metals adsorbed to microbes that are suspended in the water

column may not become concentrated in the treatment precipitates posing challenges to recovery.

Our results show that biotic HMO is more effective than abiotic HMO for adsorbing all critical metals assessed in the study. This suggests that biotic HMOs in passive treatment systems are promising targets for critical metal recovery. Optimizing microbial HMO precipitation in these systems can allow efficient remediation of Mn while promoting the adsorption and concentration of critical metals such as Co and REYs. These findings are particularly relevant to AMD discharges with high Mn content that are adjusted to circumneutral pH using passive treatment technology. At this pH, Mn is the dominant major metal, and the precipitation of HMO minerals is expected to be mediated by microbes, especially fungi.[36] Elevated Mn concentrations have been documented in coal-[26, 31, 33] and ore-related AMD discharges worldwide.[85, 86] Under these conditions, similar trends in critical metal behavior are expected.

The demand for technology and energy-critical metals is estimated to increase exponentially within the next 10 to 15 years. [35, 87, 88] There is therefore an immediate need to stabilize the global supply chain of these metals to reduce the risks of economic disruptions. [35] The elevated concentrations of REY, Co, and Mn in some AMD treatment precipitates may make them an attractive unconventional source of these critical metals that can potentially be exploited while alleviating the environmental degradation associated with traditional mining.[33] The potential economic and environmental benefits associated with using AMD treatment precipitates as critical metals feedstocks could incentivize the development of new and efficient remediation systems.

5.0 ACKNOWLEDGMENT

This work was supported by OSM Applied Science Grant to BWS and RCC, and TAO and CER were supported by the Hillman Foundation. Additional support came from an Andrew Mellon Predoctoral Fellowship and Sitler Graduate Award (University of Pittsburgh), and the Geological Society of America Graduate Student Research Grant awarded to TJBL. We thank graduate committee members E. Shelef, J. Werne, and C. Cravotta for helpful suggestions on the project, and four anonymous reviewers who provided insightful comments on an earlier version of this manuscript. We also thank J. Weitzman and H. Sinon for assisting with autoclaving and freeze drying, respectively.

6.0 REFERENCES

(1) Miyata, N.; Tani, Y.; Sakata, M.; Iwahori, K. Microbial manganese oxide formation and interaction with toxic metal ions. *Journal of bioscience and bioengineering* **2007**, *104* (1), 1-8.

(2) Villalobos, M.; Toner, B.; Bargar, J.; Sposito, G. Characterization of the manganese oxide produced by Pseudomonas putida strain MnB1. *Geochimica et Cosmochimica Acta* **2003**, *67* (14), 2649-2662.

(3) Bargar, J. R.; Fuller, C. C.; Marcus, M. A.; Brearley, A. J.; De la Rosa, M. P.; Webb, S. M.; Caldwell, W. A. Structural characterization of terrestrial microbial Mn oxides from Pinal Creek, AZ. *Geochimica et Cosmochimica Acta* **2009**, *73* (4), 889-910.

(4) Nealson, K. H.; Tebo, B. M.; Rosson, R. A. Occurrence and mechanisms of microbial oxidation of manganese. In *Advances in applied microbiology*, Vol. 33; Elsevier, 1988; pp 279-318.

(5) Brouwers, G. J.; Vijgenboom, E.; Corstjens, P.; De Vrind, J.; De Vrind-De Jong, E. Bacterial Mn2+ oxidizing systems and multicopper oxidases: an overview of mechanisms and functions. *Geomicrobiology Journal* **2000**, *17* (1), 1-24.

(6) Tebo, B. M. Manganese (II) oxidation in the suboxic zone of the Black Sea. *Deep Sea Research Part A. Oceanographic Research Papers* **1991**, *38*, S883-S905.

(7) Ehrlich, H. L. Microbes as geologic agents: their role in mineral formation. *Geomicrobiology Journal* **1999**, *16* (2), 135-153.

(8) Spiro, T. G.; Bargar, J. R.; Sposito, G.; Tebo, B. M. Bacteriogenic manganese oxides. *Accounts of Chemical Research* **2010**, *43* (1), 2-9.

(9) Li, Y.; Xu, Z.; Ma, H.; S Hursthouse, A. Removal of Manganese (II) from acid mine wastewater: A review of the challenges and opportunities with special emphasis on mn-oxidizing bacteria and microalgae. *Water* **2019**, *11* (12), 2493.

(10) Kay, J. T.; Conklin, M. H.; Fuller, C. C.; O'Day, P. A. Processes of nickel and cobalt uptake by a manganese oxide forming sediment in Pinal Creek, Globe Mining District, Arizona. *Environmental science & technology* **2001**, *35* (24), 4719-4725.

(11) Fuller, C. C.; Harvey, J. W. Reactive uptake of trace metals in the hyporheic zone of a mining-contaminated stream, Pinal Creek, Arizona. *Environmental Science & Technology* **2000**, *34* (7), 1150-1155.

(12) Moffett, J. W.; Ho, J. Oxidation of cobalt and manganese in seawater via a common microbially catalyzed pathway. *Geochimica et Cosmochimica Acta* **1996**, *60* (18), 3415-3424.

(13) Bargar, J. R.; Tebo, B. M.; Bergmann, U.; Webb, S. M.; Glatzel, P.; Chiu, V. Q.; Villalobos, M. Biotic and abiotic products of Mn (II) oxidation by spores of the marine Bacillus sp. strain SG-1. *American Mineralogist* **2005**, *90* (1), 143-154.

(14) Hausladen, D. M.; Fendorf, S. Hexavalent chromium generation within naturally structured soils and sediments. *Environmental science & technology* **2017**, *51* (4), 2058-2067.

(15) Tanaka, K.; Yu, Q.; Sasaki, K.; Ohnuki, T. Cobalt (II) oxidation by biogenic Mn oxide produced by Pseudomonas sp. strain NGY-1. *Geomicrobiology Journal* **2013**, *30* (10), 874-885.

(16) Tani, Y.; Ohashi, M.; Miyata, N.; Seyama, H.; Iwahori, K.; Soma, M. Sorption of Co (II), Ni (II), and Zn (II) on biogenic manganese oxides produced by a Mn-oxidizing fungus, strain KR21-2. *Journal of Environmental Science and Health, Part A* **2004**, *39* (10), 2641-2660.

(17) Zhao, H.; Feng, X.; Lee, S.; Reinhart, B.; Elzinga, E. J. Sorption and oxidation of Co (II) at the surface of birnessite: Impacts of aqueous Mn (II). *Chemical Geology* **2023**, 121281.

(18) Hinkle, M. A.; Dye, K. G.; Catalano, J. G. Impact of Mn (II)-manganese oxide reactions on Ni and Zn speciation. *Environmental Science & Technology* **2017**, *51* (6), 3187-3196.

(19) Zhu, M.; Farrow, C. L.; Post, J. E.; Livi, K. J.; Billinge, S. J.; Ginder-Vogel, M.; Sparks, D. L. Structural study of biotic and abiotic poorly-crystalline manganese oxides using atomic pair distribution function analysis. *Geochimica et Cosmochimica Acta* **2012**, *81*, 39-55.

(20) Webb, S. M.; Tebo, B.; Bargar, J. Structural characterization of biogenic Mn oxides produced in seawater by the marine Bacillus sp. strain SG-1. *American Mineralogist* **2005**, *90* (8-9), 1342-1357.

(21) Nelson, Y. M.; Lion, L. W.; Ghiorse, W. C.; Shuler, M. L. Production of biogenic Mn oxides by Leptothrix discophora SS-1 in a chemically defined growth medium and evaluation of their Pb adsorption characteristics. *Applied and Environmental Microbiology* **1999**, *65* (1), 175-180.

(22) Tebo, B. M.; Bargar, J. R.; Clement, B. G.; Dick, G. J.; Murray, K. J.; Parker, D.; Verity, R.; Webb, S. M. Biogenic manganese oxides: properties and mechanisms of formation. *Annu. Rev. Earth Planet. Sci.* **2004**, *32*, 287-328.

(23) Zhou, H.; Fu, C. Manganese-oxidizing microbes and biogenic manganese oxides: characterization, Mn (II) oxidation mechanism and environmental relevance. *Reviews in Environmental Science and Bio/Technology* **2020**, *19*, 489-507.

(24) Szlamkowicz, I.; Stanberry, J.; Lugo, K.; Murphy, Z.; Ruiz Garcia, M.; Hunley, L.; Qafoku, N. P.; Anagnostopoulos, V. Role of Manganese Oxides in Controlling Subsurface Metals and Radionuclides Mobility: A Review. *ACS Earth and Space Chemistry* **2022**.

(25) Ohnuki, T.; Ozaki, T.; Kozai, N.; Nankawa, T.; Sakamoto, F.; Sakai, T.; Suzuki, Y.; Francis, A. Concurrent transformation of Ce (III) and formation of biogenic manganese oxides. *Chemical Geology* **2008**, *253* (1-2), 23-29.

(26) Stewart, B. W.; Capo, R. C.; Hedin, B. C.; Hedin, R. S. Rare earth element resources in coal mine drainage and treatment precipitates in the Appalachian Basin, USA. *International Journal of Coal Geology* **2017**, *169*, 28-39.

(27) Prudêncio, M.; Valente, T.; Marques, R.; Braga, M. S.; Pamplona, J. Rare earth elements, iron and manganese in ochre-precipitates and wetland soils of a passive treatment system for acid mine drainage. *Procedia Earth and Planetary Science* **2017**, *17*, 932-935.

(28) Hedin, B. C.; Capo, R. C.; Stewart, B. W.; Hedin, R. S.; Lopano, C. L.; Stuckman, M. Y. The evaluation of critical rare earth element (REE) enriched treatment solids from coal mine drainage passive treatment systems. *International Journal of Coal Geology* **2019**, *208*, 54-64.

(29) Wallrich, I. L.; Stewart, B. W.; Capo, R. C.; Hedin, B. C.; Phan, T. T. Neodymium isotopes track sources of rare earth elements in acidic mine waters. *Geochimica et Cosmochimica Acta* **2020**, *269*, 465-483.

(30) Hedin, R. S.; Wolfe, N.; Hedin, B. Passive Removal of Mn from Mine Water Using Oxic Aggregate Beds: Results of Two Pilot Systems. *Mine Water and the Environment* **2024**, *43* (2), 255-265.

(31) Cravotta III, C. A. Dissolved metals and associated constituents in abandoned coal-mine discharges, Pennsylvania, USA. Part 1: Constituent quantities and correlations. *Applied Geochemistry* **2008**, *23* (2), 166-202.

(32) Tan, H.; Zhang, G.; Heaney, P. J.; Webb, S. M.; Burgos, W. D. Characterization of manganese oxide precipitates from Appalachian coal mine drainage treatment systems. *Applied Geochemistry* **2010**, *25* (3), 389-399.

(33) Hedin, B. C.; Hedin, R. S.; Capo, R. C.; Stewart, B. W. Critical metal recovery potential of Appalachian acid mine drainage treatment solids. *International Journal of Coal Geology* **2020**, *231*, 103610.

(34) Hedin, B. C.; Stuckman, M. Y.; Cravotta III, C. A.; Lopano, C. L.; Capo, R. C. Determination and prediction of micro scale rare earth element geochemical associations in mine drainage treatment wastes. *Chemosphere* **2023**, 140475.

(35) DOE. Critical Metal Assessement. Energy, U. S. D. o., Ed.; United States Department of Energy: 2023.

(36) Santelli, C. M.; Pfister, D. H.; Lazarus, D.; Sun, L.; Burgos, W. D.; Hansel, C. M. Promotion of Mn (II) oxidation and remediation of coal mine drainage in passive treatment

systems by diverse fungal and bacterial communities. *Applied and environmental microbiology* **2010**, *76* (14), 4871-4875.

(37) Rosenfeld, C. E.; Sabuda, M. C.; Hinkle, M. A.; James, B. R.; Santelli, C. M. A fungal-mediated cryptic selenium cycle linked to manganese biogeochemistry. *Environmental Science & Technology* **2020**, *54* (6), 3570-3580.

(38) Drits, V. A.; Lanson, B.; Gaillot, A.-C. Birnessite polytype systematics and identification by powder X-ray diffraction. *American mineralogist* **2007**, *92* (5-6), 771-788.

(39) Hinkle, M. A.; Flynn, E. D.; Catalano, J. G. Structural response of phyllomanganates to wet aging and aqueous Mn (II). *Geochimica et Cosmochimica Acta* **2016**, *192*, 220-234.

(40) Villalobos, M.; Lanson, B.; Manceau, A.; Toner, B.; Sposito, G. Structural model for the biogenic Mn oxide produced by Pseudomonas putida. *American Mineralogist* **2006**, *91* (4), 489-502.

(41) Sasaki, K.; Kaseyama, T.; Hirajima, T. Selective sorption of Co2+ over Ni2+ using biogenic manganese oxides. *Materials transactions* **2009**, *50* (11), 2643-2648.

(42) Crowther, D. L.; Dillard, J. G.; Murray, J. W. The mechanisms of Co (II) oxidation on synthetic birnessite. *Geochimica et Cosmochimica Acta* **1983**, *47* (8), 1399-1403.

(43) Drits, V. A.; Silvester, E.; Gorshkov, A. I.; Manceau, A. Structure of synthetic monoclinic Na-rich birnessite and hexagonal birnessite: I. Results from X-ray diffraction and selected-area electron diffraction. *American Mineralogist* **1997**, *82* (9-10), 946-961.

(44) Post, J. E. Manganese oxide minerals: Crystal structures and economic and environmental significance. *Proceedings of the National Academy of Sciences* **1999**, *96* (7), 3447-3454.

(45) Post, J. E.; Heaney, P. J. Neutron and synchrotron X-ray diffraction study of the structures and dehydration behaviors of ramsdellite and "groutellite". *American Mineralogist* **2004**, *89* (7), 969-975.

(46) Xu, T.; Roepke, E. W.; Flynn, E. D.; Rosenfeld, C. E.; Balgooyen, S.; Ginder-Vogel, M.; Schuler, C. J.; Santelli, C. M. Aqueous Co removal by mycogenic Mn oxides from simulated mining wastewaters. *Chemosphere* **2023**, *327*, 138467.

(47) Miyata, N.; Maruo, K.; Tani, Y.; Tsuno, H.; Seyama, H.; Soma, M.; Iwahori, K. Production of biogenic manganese oxides by anamorphic ascomycete fungi isolated from streambed pebbles. *Geomicrobiology Journal* **2006**, *23* (2), 63-73.

(48) Sasaki, K.; Matsuda, M.; Urata, T.; Hirajima, T.; Konno, H. Sorption of Co2+ ions on the biogenic Mn oxide produced by a Mn-oxidizing fungus, Paraconiothyrium sp. WL-2. *Materials Transactions* **2008**, *49* (3), 605-611.

(49) Li, Y.; Zhao, X.; Wu, J.; Gu, X. Surface complexation modeling of divalent metal cation adsorption on birnessite. *Chemical Geology* **2020**, *551*, 119774.

(50) Santelli, C. M.; Webb, S. M.; Dohnalkova, A. C.; Hansel, C. M. Diversity of Mn oxides produced by Mn (II)-oxidizing fungi. *Geochimica et Cosmochimica Acta* **2011**, *75* (10), 2762-2776.

(51) Miyata, N.; Tani, Y.; Maruo, K.; Tsuno, H.; Sakata, M.; Iwahori, K. Manganese (IV) oxide production by Acremonium sp. strain KR21-2 and extracellular Mn (II) oxidase activity. *Applied and Environmental Microbiology* **2006**, *72* (10), 6467-6473.

(52) Yin, H.; Li, H.; Wang, Y.; Ginder-Vogel, M.; Qiu, G.; Feng, X.; Zheng, L.; Liu, F. Effects of Co and Ni co-doping on the structure and reactivity of hexagonal birnessite. *Chemical Geology* **2014**, *381*, 10-20.

(53) Liu, X.; Dong, H.; Hansel, C. M. Coupled Mn (II) and Cr (III) oxidation mediated by Ascomycete fungi. *Environmental Science & Technology* **2021**, *55* (23), 16236-16245.

(54) Hinkle, M. A.; Post, J. E.; Peralta, J.; Santelli, C. M. Impacts of sulfonic acids on fungal manganese oxide production. *Geochimica et Cosmochimica Acta* **2023**, *341*, 164-182.

(55) Hansel, C. M.; Zeiner, C. A.; Santelli, C. M.; Webb, S. M. Mn (II) oxidation by an ascomycete fungus is linked to superoxide production during asexual reproduction. *Proceedings of the National Academy of Sciences* **2012**, *109* (31), 12621-12625.

(56) Zeiner, C. A.; Purvine, S. O.; Zink, E.; Wu, S.; Paša-Tolić, L.; Chaput, D. L.; Santelli, C. M.; Hansel, C. M. Mechanisms of manganese (II) oxidation by filamentous ascomycete fungi vary with species and time as a function of secretome composition. *Frontiers in Microbiology* **2021**, *12*, 610497.

(57) Tang, Y.; Zeiner, C. A.; Santelli, C. M.; Hansel, C. M. Fungal oxidative dissolution of the Mn (II)-bearing mineral rhodochrosite and the role of metabolites in manganese oxide formation. *Environmental microbiology* **2013**, *15* (4), 1063-1077.

(58) Ohta, A.; Kawabe, I. REE (III) adsorption onto Mn dioxide (δ-MnO2) and Fe oxyhydroxide: Ce (III) oxidation by δ-MnO2. *Geochimica et Cosmochimica Acta* **2001**, *65* (5), 695-703.

(59) Lefkowitz, J. P.; Elzinga, E. J. Structural alteration of hexagonal birnessite by aqueous Mn (II): Impacts on Ni (II) sorption. *Chemical Geology* **2017**, *466*, 524-532.

(60) Lefkowitz, J. P.; Elzinga, E. J. Impacts of aqueous Mn (II) on the sorption of Zn (II) by hexagonal birnessite. *Environmental science & technology* **2015**, *49* (8), 4886-4893.

(61) Wang, Y.; Benkaddour, S.; Marafatto, F. F.; Peña, J. Diffusion-and pH-dependent reactivity of layer-type MnO2: reactions at particle edges versus vacancy sites. *Environmental science & technology* **2018**, *52* (6), 3476-3485.

(62) Peña, J.; Kwon, K. D.; Refson, K.; Bargar, J. R.; Sposito, G. Mechanisms of nickel sorption by a bacteriogenic birnessite. *Geochimica et Cosmochimica Acta* **2010**, *74* (11), 3076-3089.

(63) Simanova, A. A.; Kwon, K. D.; Bone, S. E.; Bargar, J. R.; Refson, K.; Sposito, G.; Peña, J. Probing the sorption reactivity of the edge surfaces in birnessite nanoparticles using nickel (II). *Geochimica et Cosmochimica Acta* **2015**, *164*, 191-204.

(64) Sundararaju, S.; Manjula, A.; Kumaravel, V.; Muneeswaran, T.; Vennila, T. Biosorption of nickel ions using fungal biomass Penicillium sp. MRF1 for the treatment of nickel electroplating industrial effluent. *Biomass Conversion and Biorefinery* **2020**, 1-10.

(65) Cárdenas González, J. F.; Rodríguez Pérez, A. S.; Vargas Morales, J. M.; Martínez Juárez, V. M.; Rodríguez, I. A.; Cuello, C. M.; Fonseca, G. G.; Escalera Chávez, M. E.; Muñoz Morales, A. Bioremoval of cobalt (II) from aqueous solution by three different and resistant fungal biomasses. *Bioinorganic Chemistry and Applications* **2019**, *2019*.

(66) Dusengemungu, L.; Kasali, G.; Gwanama, C.; Ouma, K. O. Recent advances in biosorption of copper and cobalt by filamentous fungi. *Frontiers in Microbiology* **2020**, *11*, 582016.

(67) Díaz, A.; Marrero, J.; Cabrera, G.; Coto, O.; Gómez, J. Biosorption of nickel, cobalt, zinc and copper ions by Serratia marcescens strain 16 in mono and multimetallic systems. *Biodegradation* **2022**, 1-11.

(68) Valentine, N.; Bolton Jr, H.; Kingsley, M.; Drake, G.; Balkwill, D.; Plymale, A. Biosorption of cadmium, cobalt, nickel, and strontium by a Bacillus simplex strain isolated from the vadose zone. *Journal of industrial microbiology and biotechnology* **1996**, *16* (3), 189-196.

(69) Tanaka, K.; Tani, Y.; Takahashi, Y.; Tanimizu, M.; Suzuki, Y.; Kozai, N.; Ohnuki, T. A specific Ce oxidation process during sorption of rare earth elements on biogenic Mn oxide produced by Acremonium sp. strain KR21-2. *Geochimica et Cosmochimica Acta* **2010**, *74* (19), 5463-5477.

(70) Dhankhar, R.; Hooda, A. Fungal biosorption–an alternative to meet the challenges of heavy metal pollution in aqueous solutions. *Environmental technology* **2011**, *32* (5), 467-491.

(71) Giese, E. C. Biosorption as green technology for the recovery and separation of rare earth elements. *World Journal of Microbiology and Biotechnology* **2020**, *36*, 1-11.

(72) Sun, J.; Ji, Y.; Cai, F.; Li, J. Heavy metal removal through biosorptive pathways. *Advances in water treatment and pollution prevention* **2012**, 95-145.

(73) Markai, S.; Andres, Y.; Montavon, G.; Grambow, B. Study of the interaction between europium (III) and Bacillus subtilis: fixation sites, biosorption modeling and reversibility. *Journal of Colloid and Interface Science* **2003**, *262* (2), 351-361.

(74) Fein, J. B.; Yu, Q.; Nam, J.; Yee, N. Bacterial cell envelope and extracellular sulfhydryl binding sites: their roles in metal binding and bioavailability. *Chemical Geology* **2019**, *521*, 28-38.

(75) Liu, H.; Pourret, O.; Guo, H.; Martinez, R. E.; Zouhri, L. Impact of hydrous manganese and ferric oxides on the behavior of aqueous rare earth elements (REE): Evidence from a modeling approach and implication for the sink of REE. *International journal of environmental research and public health* **2018**, *15* (12), 2837.

(76) Davranche, M.; Pourret, O.; Gruau, G.; Dia, A.; Le Coz-Bouhnik, M. Adsorption of REE (III)-humate complexes onto MnO2: Experimental evidence for cerium anomaly and lanthanide tetrad effect suppression. *Geochimica et Cosmochimica Acta* **2005**, *69* (20), 4825-4835.

(77) Pourret, O.; Davranche, M. Rare earth element sorption onto hydrous manganese oxide: A modeling study. *Journal of colloid and interface science* **2013**, *395*, 18-23.

(78) Davranche, M.; Pourret, O.; Gruau, G.; Dia, A.; Jin, D.; Gaertner, D. Competitive binding of REE to humic acid and manganese oxide: Impact of reaction kinetics on development of cerium anomaly and REE adsorption. *Chemical Geology* **2008**, *247* (1-2), 154-170.

(79) Skousen, J. G.; Ziemkiewicz, P. F.; McDonald, L. M. Acid mine drainage formation, control and treatment: Approaches and strategies. *The Extractive Industries and Society* **2018**, *6* (1), 241-249.

(80) Skousen, J.; Zipper, C. E.; Rose, A.; Ziemkiewicz, P. F.; Nairn, R.; McDonald, L. M.; Kleinmann, R. L. Review of passive systems for acid mine drainage treatment. *Mine Water and the Environment* **2017**, *36*, 133-153.

(81) Robbins, E.; Cravotta III, C.; Savela, C.; Nord Jr, G. Hydrobiogeochemical interactions inanoxic'limestone drains for neutralization of acidic mine drainage. *Fuel* **1999**, *78* (2), 259-270.

(82) Peña, J.; Bargar, J. R.; Sposito, G. Role of bacterial biomass in the sorption of Ni by biomass-birnessite assemblages. *Environmental science & technology* **2011**, *45* (17), 7338-7344.

(83) Toner, B.; Manceau, A.; Webb, S. M.; Sposito, G. Zinc sorption to biogenic hexagonal-birnessite particles within a hydrated bacterial biofilm. *Geochimica et Cosmochimica Acta* **2006**, *70* (1), 27-43.

(84) Takahashi, Y.; Châtellier, X.; Hattori, K. H.; Kato, K.; Fortin, D. Adsorption of rare earth elements onto bacterial cell walls and its implication for REE sorption onto natural microbial mats. *Chemical geology* **2005**, *219* (1-4), 53-67.

(85) Neculita, C. M.; Rosa, E. A review of the implications and challenges of manganese removal from mine drainage. *Chemosphere* **2019**, *214*, 491-510.

(86) Royer-Lavallée, A.; Neculita, C.; Coudert, L. Removal and potential recovery of rare earth elements from mine water. *Journal of Industrial and Engineering Chemistry* **2020**, *89*, 47-57.

(87) Alonso, E.; Sherman, A. M.; Wallington, T. J.; Everson, M. P.; Field, F. R.; Roth, R.; Kirchain, R. E. Evaluating rare earth element availability: A case with revolutionary demand from clean technologies. *Environmental science & technology* **2012**, *46* (6), 3406-3414.

(88) Watari, T.; Nansai, K.; Nakajima, K. Review of critical metal dynamics to 2050 for 48 elements. *Resources, Conservation and Recycling* **2020**, *155*, 104669.

Goldschmidt International Geochemistry Conference
July 9-14, 2023 – Lyon, France

EXPERIMENTAL INVESTIGATION OF CRITICAL METAL REMOVAL BY BIOTIC MANGANESE OXIDES

Tashane Boothe[1], Rosemary Capo[1], Brian Stewart[1], Carla Rosenfeld[2]
[1] *Department of Geology and Environmental Science, University of Pittsburgh, Pittsburgh, PA 15260*

[2]*Carnegie Museum of Natural History, Pittsburgh, PA 15213*

Abstract

Ore grade concentrations of energy critical metals have been identified in the precipitate by-products from some acid mine drainage (AMD) treatment systems that utilize microbially-mediated oxidation (passive) technology. These metals are often disproportionately associated with manganese oxides and hydroxides (collectively referred to as MnO_x) through adsorption and/or coprecipitation.[1]

To understand the conditions that facilitate critical metal enrichment in passive AMD treatment systems, we investigated the attenuation of ten critical metals (Co, Ni, La, Ce, Nd, Pr, Gd, Dy, Yb, and Y) in solutions with and without MnO_x produced by two fungal species, *Paraphaeosphaeria sporulosa* (previously *Paraconiothyrium sporulosum)* and *Stagonospora* sp. These species are known to produce forms of MnO_x such as δ-MnO_2 or acid birnessite that are highly disordered and have a high adsorption capacity.[2] In our experiment, critical metals were allowed to interact with the biotic MnO_x and fungal biomass for 31 days with periodic sampling to assess critical metal removal by the minerals and/or biomass. Control experiments were also conducted to assess the behavior of critical metals with no MnO_x or biomass present, and with fungal biomass only.

Our results indicate that the fungi differ in their capacity to oxidize manganese. *Stagonospora sp.* oxidized 99% of Mn in solution after 14 days, whereas *P. sporulosa* oxidized 60% of Mn over the same period. The critical metal removal capacity also varied between the two fungal species. Cobalt in solution decreased by 90% and 80% in the presence of MnO_x produced by *Stagonospora* sp. and *P. sporulosa,* respectively. For both fungi, Co removal from solution was 30% greater than Ni removal after 31 days. Near total rare earth element (REE) and Y removal was achieved (95% - 99%) within 18 days, both in the presence of biotic MnO_x and with fungal biomass only. Normalized REE patterns show a preferential removal of light REE over 31 days with little to no apparent Ce anomaly.

[1] Hedin B. C. et al. (2019). *Int. Jour. Coal Geol. 208*, 54-64.
[2] Rosenfeld C. E. et al. (2020). *Env. Sci. Technol. 54*, 3570-3580.

GSA Connects 2023 Meeting in Pittsburgh, Pennsylvania

Paper No. 29-7
Presentation Time: 8:00 AM-5:30 PM

A COMPARATIVE ASSESSMENT OF CRITICAL METAL REMOVAL BY BIOTIC AND ABIOTIC HYDROUS MANGANESE OXIDES

BOOTHE, Tashane Jessica[1], CAPO, Rosemary C.[1], STEWART, Brian[1] and ROSENFELD, Carla[2], (1)Department of Geology and Environmental Science, University of Pittsburgh, Pittsburgh, PA 15260, (2)Carnegie Museum of Natural History, Pittsburgh, PA 15213

Microbial (biotic) oxidation of Mn can produce a wide variety of hydrous manganese oxides (HMOs) with high cation adsorption capacity. In passive acid mine drainage (AMD) treatment systems, biotic HMO may dominate over abiotic HMO, resulting in treatment precipitates with high concentrations of energy-critical metals such as rare earth elements (REE), Co, and Ni **[1]**. To understand the relative importance of abiotic and biotic processes in passive treatment systems, we conducted benchtop experiments to investigate the uptake of ten critical metals (Co, Ni, La, Ce, Nd, Pr, Gd, Dy, Yb, and Y) by (1) HMOs produced by two fungal species (*Paraphaeosphaeria sporulosa* and *Stagonospora* sp.) and (2) abiotic HMO, vernadite (δ-MnO_2), synthesized using a method described by Hinkle et al. **[2]**. Experiments involving the abiotic HMO are currently underway to assess critical metal uptake and to allow comparative analyses of biotic and abiotic uptake rates and efficiency.

Preliminary results of the biotic experiments show that in the presence of dissolved Mn, both fungi produced a highly disordered HMO similar to vernadite which becomes more ordered and crystalline with time. However, *Stagonospora* sp. was more efficient at removing dissolved Mn from solution compared to *P. sporulosa.* Critical metal uptake by biotic HMO (HMO + fungal biomass) and fungal biomass only was assessed via periodic sampling over 31 days to track changes in dissolved metal concentrations. Our results indicate that Co in solution decreased by 90% and 80% in the presence of HMO produced by *Stagonospora* sp. and *P. sporulosa,* respectively. In contrast, only 50-60% of Ni was removed after 31 days. The presence of fungal biomass only did not result in significant removal of Co and Ni. Near total removal (95-99%) of REE and Y was achieved within 18 days, both in the presence of biotic HMO and fungal biomass only. Normalized REE patterns show a preferential removal of light REE over 31 days with no apparent Ce anomaly.

[1] Hedin, BC et al., 2019, Int. J. Coal Geol. 208, 54-64. **[2]** Hinkle, MA et al., 2016, Geochim. Cosmochim. Acta 192, 220-234.

Session No. 29--Booth# 116

T10. Characterization of Critical Metals in Unconventional Ores to Inform Recovery Potential (Posters)
Sunday, 15 October 2023: 8:00 AM-5:30 PM

Hall B (David L Lawrence Convention Center)

Geological Society of America *Abstracts with Programs.* Vol. 55, No. 6
doi: 10.1130/abs/2023AM-395500

Back to: T10. Characterization of Critical Metals in Unconventional Ores to Inform Recovery Potential (Posters)

<< Previous Abstract | Next Abstract >>

213-1 - EMPIRICAL OBSERVATIONS AND GEOCHEMICAL MODELING TO EVALUATE TREATMENT STRATEGIES FOR RECOVERY OF RARE-EARTH ELEMENTS FROM ACID MINE DRAINAGE *(Invited)*

Wednesday, 18 October 2023

8:05 AM - 8:25 AM

324 (3, David L Lawrence Convention Center)

Abstract

The lanthanide rare-earth elements, yttrium, and scandium (REYs) generally occur at elevated concentrations in acid mine drainage (AMD) with low pH and elevated concentrations of Fe, Al, and SO_4. This study explains why concentrations of REYs and associated trace metals in AMD generally decrease as pH increases, particularly at pH > 5, and employs geochemical models to demonstrate the importance of key variables. Laboratory and field studies demonstrate that REYs are attenuated with metal-rich solids precipitated during neutralization of AMD, and that attenuation is enhanced by SO_4. Geochemical modeling indicates that observations can be explained by adsorption of REYs to hydrous ferric oxide (HFO), hydrous aluminum oxide (HAO), and/or hydrous manganese oxide (HMO). New, empirically derived adsorption reactions and associated equilibrium constants for binding of REYs cations (M^{+3}) by HFO, HAO, and HMO plus sulfate complexes (MSO_4^{+}) by HFO and HAO account for effects of SO_4. The PHREEQ-N-AMDTreat+REYs water-quality modeling tools (https://doi.org/10.5066/P9M5QVK0), which incorporate these and other speciation reactions, accurately simulate the precipitation of Fe, Al, and Mn solids during sequential AMD treatment steps, plus the precipitation and adsorption of REYs. Each model has a user interface to facilitate the input of water-quality data and adjustment to geochemical or treatment system variables. On-screen graphs display predicted changes in REYs and associated solute concentrations as functions of pH or retention time; details are summarized in output tables. A goal of such modeling is to identify strategies that could produce a concentrated REYs extract from AMD or mine waste leachate. For example, modeling supports the hypothesis that Fe can be removed at pH < 4 using conventional sequential oxidation and neutralization treatment processes without removing REYs and that further increasing pH can promote the adsorption of REYs by HFO, HAO, or HMO that forms thereafter. Alternatively, chemicals such as phosphate or oxalate may be added to precipitate REYs compounds following steps to decrease non-target metal concentrations. The PHREEQ-N-AMDTreat+REYs models will be incorporated as new tools in the AMDTreat 6.0 cost-analysis model by the Office of Surface Mining Reclamation and Enforcement.

Geological Society of America Abstracts with Programs. Vol. 55, No. 6, 2023
doi: 10.1130/abs/2023AM-392405

Author

C

Charles Cravotta
Pennsylvania Water Science Center

Authors

T

Travis L. Tasker
Saint Francis University

H

Benjamin C. Hedin
Hedin Environmental

View Related

American Geophysical Union Annual Meeting
December 11-15, 2023 – San Francisco, California

Critical element (REE, Co, Ni) sorption by biotic and abiotic hydrous manganese oxides relevant to **AMD treatment systems**

Tashane Boothe[1], Rosemary Capo[1], Brian Stewart[1], Carla Rosenfeld[2]
[1] Department of Geology and Environmental Science, University of Pittsburgh, Pittsburgh, PA 15260
[2]Carnegie Museum of Natural History, Pittsburgh, PA 15213

Abstract (1970/max 2000 characters, excluding spaces)

Mine drainage remediation systems can sequester >90% of dissolved rare earth elements (REE) and other critical metals in solids precipitated during treatment **[1]**. Reactive minerals such as hydrous manganese oxides (HMO) are known to control the solubility, transport, and bioavailability of metals and organic compounds in soil, sediments, and water through oxidation and sorption **[2]**, and high concentrations of energy-critical metals (e.g. REE, Co, and Ni) in passive acid mine drainage (AMD) treatment system solids have been linked to biogenic HMO phases **[1].** To understand the relative importance of biotic and abiotic HMOs in AMD treatment systems, we are conducting benchtop experiments to assess the uptake of ten critical metals (Co, Ni, La, Ce, Nd, Pr, Gd, Dy, Yb, and Y) by (1) biogenic HMO produced by two fungal species present in AMD treatment systems (*Paraphaeosphaeria sporulosa* and *Stagonospora* sp and (2) abiotic vernadite (δ-MnO_2) and H+ birnessite, synthesized using a method described by Hinkle et al. **[3]**.

Preliminary results indicate that the fungi differ in their capacity to oxidize manganese and over a 14-day period, *Stagonospora* sp. was more efficient at removing dissolved Mn from solution compared to *P. sporulosa*. XRD analysis indicates that in the presence of dissolved Mn, both produced a disordered, poorly crystalline HMO similar to vernadite; crystallinity increased with time. Critical metal uptake by biotic HMO (HMO+ fungal biomass) and fungal biomass only was assessed via periodic sampling. After 31 days, fungal biomass alone did not result in significant removal of Co or Ni. However, Co in solution decreased by 80% (*P. sporulosa*) to 90% (*Stagonospora* sp) in the presence of biogenic HMO and 50-60% of Ni was removed during that time. Normalized REE patterns show a preferential removal of light REE over 31 days with no apparent Ce anomaly, with near total removal (95-99%) of REE and Y achieved within 18 days, both in the presence of biotic HMO and by fungal biomass only.

[1] Hedin, BC et al., 2019, Int. J. Coal Geol. 208, 54-64. **[2]** Kay, JT et al., 2001,. Env. Sci. & Tech. 35 (24), 4719-4725. **[3]** Hinkle, MA et al., 2016, Geochim. Cosmochim. Acta 192, 220-234.

Lab-based assessment of critical metal adsorption by biotic and abiotic hydrous manganese oxides

Tashane J. Boothe[1], Rosemary C. Capo[1], Brian W. Stewart[1], Benjamin C. Hedin[2], Travis A. Olds[3], Carla E. Rosenfeld[3]

[1]*Department of Geology and Environmental Science, University of Pittsburgh, Pittsburgh, PA 15260*

[2]*Hedin Environmental, 195 Castle Shannon Blvd., Pittsburgh, PA 15228*

[3]*Carnegie Museum of Natural History, Pittsburgh, PA 15213*

Extended Abstract

The global demand for technology and energy critical minerals is expected to increase in the coming years (Alonso et al. 2012). Developing new and sustainable sources of these metals will stabilize supply and alleviate the potential pollution produced by traditional mining. Acid mine drainage (AMD) treatment precipitates are a potential source of critical metals, including Ni, Mn, Co, and rare earth elements (REE) (Cravotta, 2008; Ayora, et al., 2016; Stewart et al., 2017; Vass, et al., 2019). Hydrous manganese oxides (HMO), common constituents of AMD treatment precipitates, are known to be very efficient at sorbing and concentrating trace metals (Tan et al., 2010; Hedin et al., 2019; 2023). However, more work is needed to understand how the biogeochemical conditions within AMD treatment systems influence HMO formation and their ability to adsorb and concentrate critical metals.

In this study we performed bench-top experiments to investigate the sorption of critical metals (La, Nd, Ce, Gd, Pr, Dy, Yb, Y, Co, and Ni) by biotically- and abiotically-precipitated HMO. The biotic HMO was produced through the oxidation of $MnCl^2$ by two species of Mn-oxidizing fungi, *P. sporulosa* and *Stagonospora sp.*, and the abiotic HMO (δ-MnO^2 and H^+ birnessite) were synthesized through chemical oxidation of aqueous $MnCl_2$. The efficiency of critical metal uptake by these HMO was assessed by conducting time series analyses of dissolved metal concentrations over 31 days and by characterizing the HMO minerals.

Scanning electron microscopy shows that HMO produced by *Stagonospora sp.* and *P. sporulosa* are closely associated with fungal biomass and hyphae. X-ray diffraction shows that both biotic and abiotic HMO were initially poorly crystalline, but abiotic HMO transformed to more crystalline HMO phases over the 31 days of the experiment. Biotic HMO and/or fungal biomass facilitate rapid adsorption of REE. After 6 hours, greater than 99% of both LREE and HREE were removed from solution (Fig. 1). The LREE were preferentially adsorbed, and the Ce anomaly was weak or absent. Biotic HMO also adsorbed 80-90% of dissolved Co and 50–60% of dissolved Ni from solution over 31 days. Energy-dispersive X-ray spectroscopy confirms that critical metals become associated with both HMO and fungal biomass. Abiotic HMO adsorbed REE at a slower rate, with maximum adsorption occurring after 4 days. After 31 days, 75–80% and 50–70% of LREE and HREE, respectively, were adsorbed. However, abiotic HMO only adsorbed 5–10% of Co and Ni over the same timeframe.

This study shows that biotic HMO are very efficient at adsorbing critical metals. Fungal biomass also plays an important role in this process. Abiotic HMO may be susceptible to mineral transformation and dissolution under certain conditions, and this can potentially reduce their capacity to adsorb some critical metals. AMD treatment systems that produce HMO through microbial oxidation (passive systems) are therefore likely viable targets for critical metal recovery.

Keywords: HMO, critical metals, REE, cobalt, nickel, fungi, acid mine drainage

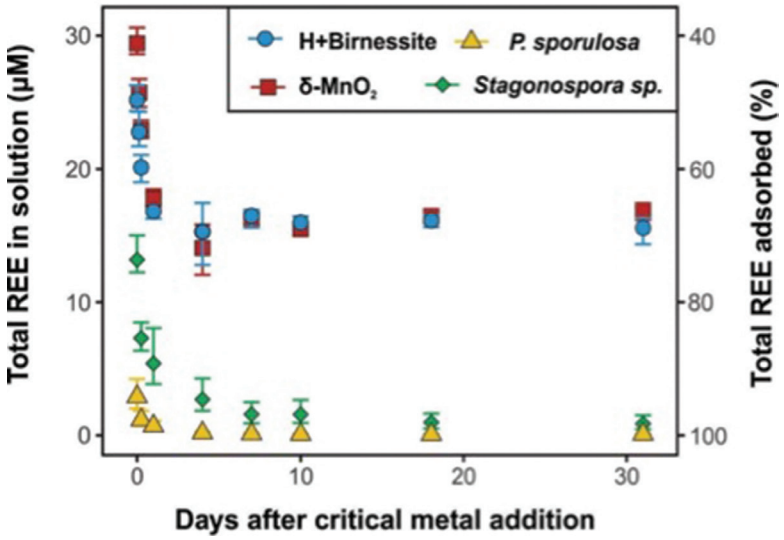

Figure 1 *Change in total REE concentration over 31 days after the addition of critical metals in the presence of biotic HMO produced by Stagonospora sp. and P. sporulosa, and abiotic HMO δ-MnO_2 and H^+ birnessite*

Acknowledgements

The authors thank the anonymous reviewer who provided comments on the earlier version of text. This work is supported by a Geological Society of America Graduate Student Research Grant (TB), a DOI-Office of Surface Mining Applied Science award (BWS, RCC) and the Carnegie Museum of Natural History (CR, TO).

References

Alonso E, Sherman AM, Wallington TJ, Everson MP, Field FR, Roth R, Kirchain RE (2012) Evaluating rare earth element availability: A case with revolutionary demand from clean technologies. Environ. Sci. & Tech. 46(6): 3406-3414, doi.org/10.1021/es203518d

Ayora C, Macias F, Torres E, Lozano A, Carrero S, Nieto JM, Perez-Lopez R, Fernandez-Martinez A, Castillo-Michel H (2016) Recovery of rare earth elements and yttrium from passive-remediation systems of acid mine drainage. Environ. Sci. Technol. 50: 8255-8262, doi.org/10.1021/acs.est.6b02084

Cravotta, C.A., III (2008) Dissolved metals and associated constituents in abandoned coal-mine discharges, Pennsylvania, USA. Part 2: Geochemical controls on constituent concentrations. Appl. Geochem. 23: 203-226

Hedin BC, Capo RC, Stewart BW, Hedin RS, Lopano CL, Stuckman MY (2019) The evaluation of critical rare earth element (REE) enriched treatment solids from coal mine drainage passive treatment systems. Int. Jour. of Coal Geol. 208: 54-64, doi.org/10.1016/j.coal.2019.04.007

Hedin, BC, Stuckman, MY. Cravotta III, CE, Lopano, CL, Capo, RC (2023) Determination and prediction of micro-scale rare earth element geochemical associations in mine drainage treatment wastes, Chemos. 346: 140475, doi.org/10.1016/j.chemosphere.2023.140475.

Stewart BW, Capo RC, Hedin BC, Hedin RS (2017) Rare earth element resources in coal mine drainage and treatment precipitates in the Appalachian Basin, USA. Int. Jour. of Coal Geol. 169: 28-39, doi.org/10.1016/j.coal.2016.11.002

Tan H, Zhang G, Heaney PJ, Webb SM, Burgos WD (2010) Characterization of manganese oxide precipitates from Appalachian coal mine drainage treatment systems. App. Geoch. 25 (3): 389-399, doi.org/10.1016/j.apgeochem.2009.12.006

Vass CR, Noble A, Ziemkiewicz PF (2019) The occurrence and concentration of rare earth elements in acid mine drainage and treatment by-products: Part 1—Initial survey of the northern Appalachian Coal Basin. Mining Metal. Explor. 36: 903-916, doi.org/10.1007/s42461-019-00112-9

Laboratory and Field Observations Inform Geochemical Models of Treatment Strategies to Recover Rare-Earth Elements from Acid Mine Drainage

Charles A. Cravotta III[1], Travis L. Tasker[2], Benjamin C. Hedin[3]

[1]*Cravotta Geochemical Consulting, Bethel, PA, USA, cravottageochemical@gmail.com, ORCID 0000-0003-3116-4684*

[2]*Saint Francis University, Loretto, PA, USA, ttasker@francis.edu, ORCID 0000-0001-5040-7579*

[3]*Hedin Environmental, Inc., Pittsburgh, PA, USA, ben.hedin@hedinenv.com, ORICID 0000-0002-4695-9634*

Extended Abstract

Discharges from coal mines that have low pH, hereinafter identified as acid mine drainage (AMD), commonly have elevated dissolved concentrations of sulfate (SO_4), transition metals (Fe > Mn > Zn > Ni > Co > Cu > Cr > Cd), other metals (Al > Pb > Ga > Tl > In), and the lanthanide rare-earth elements, yttrium, and scandium (REYs: Y > Ce > Sc > Nd > La > Gd > Dy > Sm > Pr > Er > Yb > Eu > Ho > Tb > Tm > Lu) (Cravotta, 2008a). The REYs and many of these associated metals are among more than 50 "critical minerals" that are in great demand for clean energy and other modern technologies and for which global supply chains are vulnerable to disruption (Schulz et al. 2017; Nassar et al. 2020). The REYs occur as trace cations having predominant 3+ oxidation state (Me^{3+}) in AMD and associated waters, with tendency to form aqueous and surface complexes (Verplanck et al. 2004; Pourret and Davranche, 2013; Liu et al. 2017; Lozano et al. 2019). Dissolved REYs concentrations in AMD generally decrease as the pH increases, especially at pH > 5, accumulating with Fe, Al, and Mn that precipitate as hydrous metal oxides (HMeO) (Verplanck et al. 2004; Cravotta, 2008a; Vass et al. 2019a, 2019b; Hedin et al. 2020, 2024) (Fig. 1). In contrast, the concentration of dissolved SO_4, the predominant anion in AMD, tends to remain elevated and largely uncomplexed across a wide range of pH, despite limited precipitation with Fe and Al hydroxysulfate compounds (e.g. jarosite, schwertmannite, basaluminite) (Cravotta, 2008a, 2008b; Nordstrom, 2020) and/or adsorption by hydrous Fe, Al, and/or Mn oxides (Dzombak and Morel, 1990; Yao and Millero, 1996; Karamalidis and Dzombak, 2010; Lozano et al. 2019).

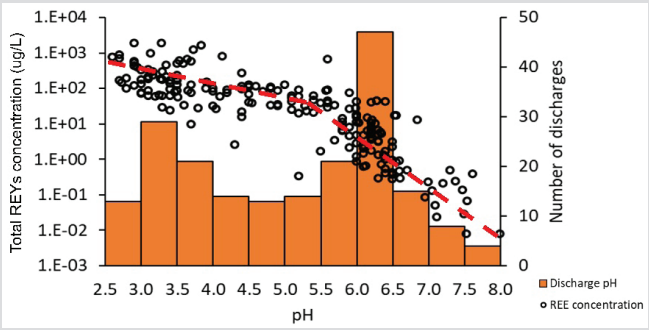

Figure 1 *Rare-earth elements (REYs) are elevated in AMD from coal mines in Pennsylvania (adapted from Cravotta, 2008a; Hedin et al. 2020). Dissolved REYs concentrations decrease with increased pH, exhibiting a break in slope at pH ≈5. The REYs accumulate with Fe, Mn, and Al in AMD treatment solids*

An economically sustainable approach for recovery of REYs and other associated critical minerals from AMD could offset treatment costs, depending on environmental and economic factors for extraction and transport (Fritz et al. 2021). Various AMD treatment strategies may be effective for concentrating REYs with AMD treatment solids through adsorption and/or precipitation with hydroxide, phosphate, or oxalate compounds (Ayora et al. 2016; Zhang and Honaker, 2018; Josso et al. 2018; Edahbi et al. 2018; Royer-Lavallée et al. 2020; Wang et al. 2021; Leon et al. 2021; Mwewa et al. 2022; Hermassi et al. 2022). Nevertheless, impurities such as Fe, Al, Mn, Ca, and Mg, which are major components in typical AMD treatment solids (Hedin et al. 2020, 2024; Wang et al. 2021), tend to dilute the concentrations of more valuable trace components, increasing costs for transportation and processing. If REYs could be concentrated after first removing Fe and Al, without addition or precipitation of Mg and Ca, subsequent REYs-bearing fluids or solid(s) may have greater value for REYs recovery.

This study employs version 1.0.3 of the PHREEQ-N-AMDTreat+REYs water-quality modeling tools (Cravotta, 2022), which were expanded from the original PHREEQ-N-AMDTreat tools (Cravotta, 2021) to simulate changes in the concentrations of REYs, Fe, Al, Mn, SO_4, and other solutes plus the formation of solids containing REYs. The models simulate the evolution of AMD in response to treatment, considering the composition and availability of HMeO sorbent and the potential for REYs compounds and other solids to precipitate. The models utilize the wateq4fREYsKinetics.dat database, which was expanded from wateq4f.dat (Ball and Nordstrom, 1991) provided with PHREEQC (Parkhurst and Appelo, 2013) to include thermodynamics data on REYs aqueous and surface species plus relevant REYs solid phases (hydroxide, carbonate, phosphate, and oxalate compounds). Surface species for REYs plus other cations and anions were added for hydrous ferric oxide (HFO: Dzombak and Morel, 1990), hydrous aluminum oxide (HAO: Karamalidis and Dzombak, 2010; Lozano et al. 2019), and hydrous manganese oxide (HMO: Tonkin et al. 2004; Pourret and Davranche, 2013), which constitute the total HMeO sorbent mass.

To investigate potential effects of sorbent composition, pH, and SO_4, a series of titration experiments was recently conducted in the laboratory during summer 2022. Each experiment used a solution with starting pH less than 2 that contained 50 µg/L of each of the 16 REYs plus 1 mmol/L of sorbent metal (Fe, Al, or Mn). To evaluate if REYs attenuation resulted by co-precipitation with Fe, Al, or Mn versus adsorption by HFO, HAO, or HMO, replicate experiments were conducted in parallel using the same REYs concentrations with initially aqueous (Fe^{3+}, Al^{3+}, or Mn^{3+}) or solid (HFO, HAO, or HMO) forms. A hydrochloric acid (HCl) solution matrix was used for the first set of experiments, whereas a sulfuric acid (H_2SO_4) solution was used for the other sets of experiments. For all experiments, the pH was increased to pH values ranging from about 3 to 10 by titration with sodium hydroxide (NaOH). The dissolved concentrations of REYs and major metals were measured after 24 hours reaction time, centrifuging, and filtration (0.45-µm).

To model the empirical titration results, new adsorption reactions and equilibrium constants were estimated using PEST version 17.5 (Doherty, 2015) in combination with PHREEQC (Parkhurst and Appelo, 2013). Instead of using estimates from linear free energy relations (LFER) for divalent cations, we (1) adapted the adsorption expression for Cr^{3+}, the only trivalent cation reported by Dzombak and Morel (1990) (eq. 5), and also (2) determined new equilibrium constants for reactions where the uncomplexed cation is bound by adsorbed SO_4 (eq. 7) (Table 1).

Speciation models using PHREEQC with the new adsorption expressions (eqs. 5 and 7) accurately describe the observed adsorption of REYs to HFO (Fig. 2, bottom graphs). In contrast, modeled adsorption using equilibrium constants estimated by LFER (eq. 4)

Table 1 *Aqueous and surface speciation reactions considered in PHREEQ-N-AMDTreat+REYs models*

Aqueous speciation reactions (Me^{+n} is divalent (n=2) or trivalent (n=3) cation):		
$Me^{+n} + H_2O = MeOH^{(n-1)} + H^+$	$LogK_{OH}\ MeOH_1$	(eq. 1)
$Me^{+n} + SO_4^{-2} = Me(SO_4)^{(n-2)}$	$LogK_S\ MeSO_4$	(eq. 2)
Surface speciation reactions (SURF is HFO, HAO, or HMO):		
$SURF\_OH + SO_4^{-2} = SURF\_OHSO_4^{-2} + H^+$	$Log\ K_1\ SURF\_OHSO_4^{-2}$	(eq. 3)
$SURF\_OH + Me^{+n} = SURF\_OMe^{(n-1)} + H^+$ (LFER)	$Log\ K_2\ SURF\_OMe^{(n-1)}$	(eq. 4)
$SURF\_OH + Me^{+n} + H_2O = SURF\_OMeOH^{(n-2)} + 2H^+$	$Log\ K_3\ SURF\_OHMe^{(n-2)}$	(eq. 5)
$SURF\_OH + Me(SO_4)^{(n-2)} = SURF\_OMe(SO_4)^{(n-3)} + H^+$	$Log\ K_4\ SURF\_OMe(SO_4)^{(n-3)}$	(eq. 6)
$SURF\_OHSO_4^{-2} + Me^{+n} = SURF\_OMe(SO_4)^{(n-3)} + H^+$	$Log\ K_5\ SURF\_OMe(SO_4)^{(n-3)}$	(eq. 7)

Note that equation 4 is widely applied for divalent cations and to estimate adsorption equilibrium constants given the first hydrolysis constant (eq. 1) and linear free energy relation (LFER) expressions. Also, note that equation 7 is derived by subtracting equation 3 from the sum of equations 2 and 6 ($Log\ K_5 = Log\ K_4 + Log\ K_S - Log\ K_1$)

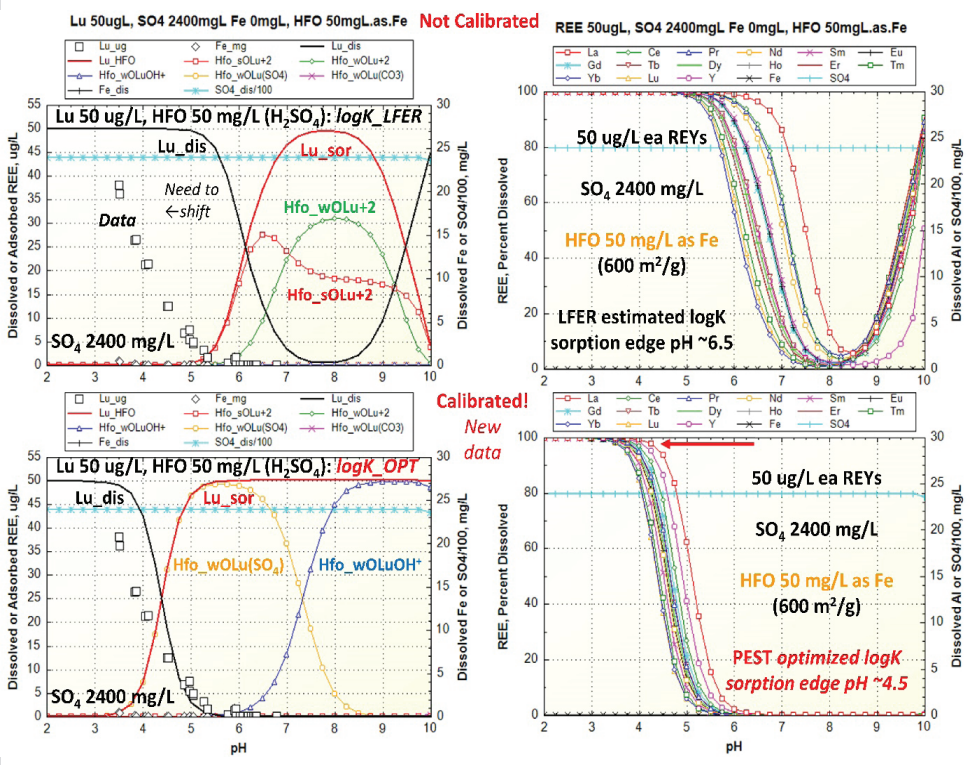

Figure 2 *Model calibration to empirical data. Graphs on the left show lutetium attenuation by HFO slurry in sulfuric acid matrix. The top graph shows poor fit of the initial model based on LFER estimated log K values (eq. 3); the lower graph shows results using the "best-fit" adsorption log K values derived using PEST and new equilibrium expressions for trivalent cations that consider effects of pH and SO_4 (eqs. 5, 6, 7). On the right, model curves are shown for all 16 REYs. The upper graph shows initial results using LFER estimates. The lower graph shows results using the new optimized log K values. The empirical data and model results indicate effective pH of adsorption shifted by 2 pH units from approximately 6.5 (LFER) to 4.5 (optimized)*

greatly underestimated the observed attenuation of REYs at pH <6, especially in the presence of SO_4 (Fig. 2, top graphs). The new model results are consistent with prior reports for AMD systems where ternary complexes with SO_4 resulted in enhanced adsorption of various divalent cations (Me^{2+}: Cd, Cu, Co, Pb, Ni, Zn) by HFO (Swedlund and Webster, 2001; Swedlund et al. 2003) and trivalent REYs (Me^{3+}) by HAO (Lozano et al. 2019). Therefore, version 1.0.3 of PHREEQ-N-AMDTreat+REYs (Cravotta, 2022) includes the new equilibrium reactions for adsorption of Me^{2+} and Me^{3+} by HFO, HAO, and HMO plus interactions of those cations as with adsorbed SO_4 ($HFO\_SO_4^{-2}$ and $HFO\_SO_4^{-2}$).

Potential treatment strategies that could feasibly produce a concentrated REYs extract from AMD are evaluated using PHREEQ-N-AMDTreat+REYs models. For a passive treatment case, Hedin et al. (2024) reported REYs accumulated in limestone beds can be accurately simulated using the "CausticTitrationMix2.exe" tool, which indicated attenuation of REYs mainly with HAO and HMO. For an active treatment case, a coal-refuse facility with highly acidic leachate having elevated concentrations of Fe, Al, Mn, and REYs currently utilizes lime neutralization, which causes precipitation of Fe, Al, and REYs into complex Fe-Al-Ca rich sludge mixture. The current treatment and two alternative strategies that could concentrate REYs were simulated with the "TreatTrainMix2REYs.exe" tool (Fig. 3). The lime treatment to pH ≈8.7 removes REYs with the sludge mixture. In contrast, alternative strategies using H_2O_2 to oxidize Fe^{II} demonstrate potential for removal of most Fe and Al without substantial removal of REYs. In one case, NaOH is added to initial pH 3 followed by aeration to precipitate Fe and Al oxyhydroxides at pH <4.5. Subsequent aeration and further increasing pH with limestone promotes adsorption of REYs by HAO and HMO that form thereafter. In another case, NaOH and NaH_2PO_4 are added to precipitate REY-PO_4 after H_2O_2 addition (e.g. Hermassi et al. 2022). In both cases, REYs-enriched solids produced by the alternative treatments contain a small fraction of the initial Fe and Al and most of the REYs. Bench-scale testing of the simulated, sequential treatment steps to concentrate REYs into solids may be considered, guided by modeling, to verify results and evaluate extraction methods to re-mobilize the REYs from the various solid components (e.g. Rushworth et al. 2023; Boothe et al. 2024).

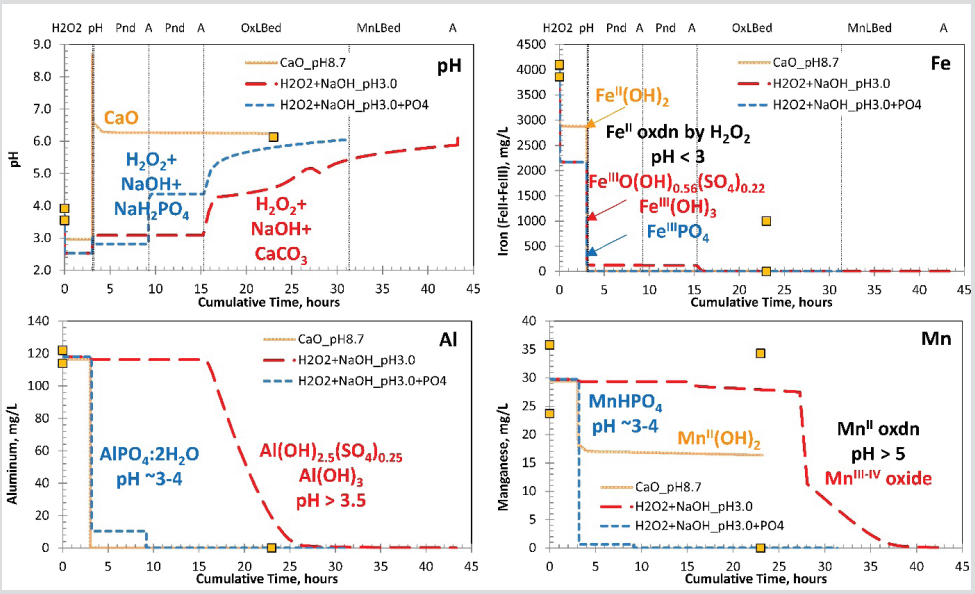

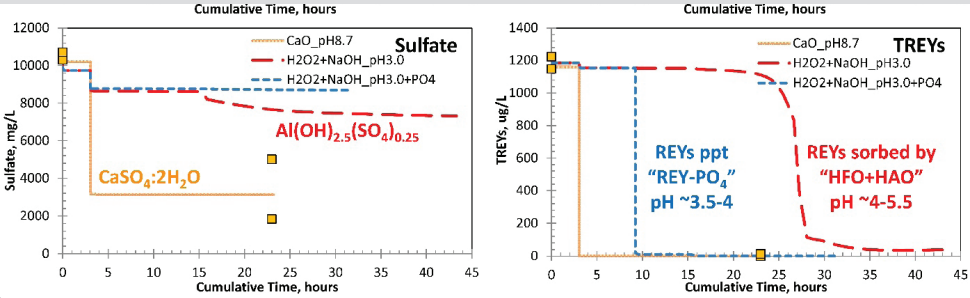

Figure 2 *Comparison of measured (symbols) and PHREEQ-N-AMDTreat+REYs simulation results (curves) for pH and dissolved Fe, Al, Mn, SO_4, and total REYs concentrations at a coal-refuse disposal facility. Measured values are for lime treatment without H_2O_2, sampled on two different dates*

By combining the PHREEQ-N-AMDTreat+REYs water-quality modeling tools with the AMDTreat 6.0 cost-analysis model (Office of Surface Mining Reclamation and Enforcement, 2022), a user may (1) identify and evaluate strategies for AMD treatment that result in effective REYs recovery and (2) estimate costs for installation and operation of relevant treatment steps.

Keywords: Resource recovery, rare-earth elements, adsorption, aqueous speciation, PHREEQC, AMDTreat

Acknowledgements

Financial support for the PHREEQ-N-AMDTreat-+REYs software and laboratory adsorption experiments was provided by the Office of Surface Mining Reclamation and Enforcement. Charles Cravotta retired from the U.S. Geological Survey (USGS) in December 2023. Although the PHREEQ-N-AMDTreat+REYs software has been approved for release by the USGS, this paper has not been subjected to USGS review and approval.

References

Ayora C, Macías F, Torres E, Lozano A, Carrero S, Nieto JM, Pérez-López R, Fernández-Martínez A, Castillo-Michel H (2016) Recovery of rare earth elements and yttrium from passive-remediation systems of acid mine drainage. Environ Sci Tech 50:8255-8262. https://doi.org/10.1021/acs.est.6b02084

Ball JW, Nordstrom DK (1991) User's manual for WATEQ4F, with revised thermodynamic data base and test cases for calculating speciation of major, trace, and redox elements in natural waters. US Geol Surv Open-File Report 91-183. https://pubs.usgs.gov/of/1991/0183/report.pdf

Boothe TJ, Capo RC, Stewart BW, Hedin B, Olds T, Rosenfeld C (2024) Lab-based assessment of critical metal adsorption by biotic and abiotic hydrous manganese oxides. 2024 West Virginia Mine Drainage Task Force Symposium & 15th International Mine Water Association Congress (this proceedings).

Cravotta CA III (2008a) Dissolved metals and associated constituents in abandoned coal-mine discharges, Pennsylvania, USA -- 1. Constituent concentrations and correlations. Appl Geochem 23:166-202. https://dx.doi.org/10.1016/j.apgeochem.2007.10.011

Cravotta CA III (2008b) Dissolved metals and associated constituents in abandoned coal-mine discharges, Pennsylvania, USA -- 2. Geochemical controls on constituent concentrations. Appl Geochem 23:203-226. https://dx.doi.org/10.1016/j.apgeochem.2007.10.003

Cravotta CA III (2021) Interactive PHREEQ-N-AMDTreat water-quality modeling tools to evaluate performance and design of treatment systems for acid mine drainage. Appl Geochem 126:104845. https://doi.org/10.1016/j.apgeochem.2020.104845

Cravotta CA III (2022) Interactive PHREEQ-N-AMDTreat+REYs water-quality modeling tools to evaluate potential attenuation of rare-earth elements and associated dissolved constituents

by aqueous-solid equilibrium processes (software download). US Geol Surv Software Release https://doi.org/10.5066/P9M5QVK0

Doherty J (2015) Calibration and uncertainty analysis for complex environmental models. PEST: complete theory and what it means for modeling the real world. Watermark Numerical Computing, Brisbane, Australia. https://pesthomepage.org/pest-book

Dzombak DA, Morel FMM (1990) Surface complexation modeling: Hydrous ferric oxide. John Wiley and Sons, New York, NY, USA.

Edahbi E, Plante B, Benzaazoua M, Ward M, Pelletier M (2018) Mobility of rare earth elements in mine drainage: Influence of iron oxides, carbonates, and phosphates. Chemosphere 199:647-654. https://doi.org/10.1016/j.chemosphere.2018.02.054

Fritz AG, Tarka TJ, Mauter MS (2021) Technoeconomic assessment of a sequential step-leaching process for rare earth element extraction from acid mine drainage precipitates. ACS Sustainable Chem Engineer 9:9308-9316. https://doi.org/10.1021/acssuschemeng.1c02069

Hedin BC, Hedin RS, Capo RC, Stewart BW (2020) Critical metal recovery potential of Appalachian acid mine drainage treatment solids. Int J Coal Geol 231:103610. https://doi.org/10.1016/j.coal.2020.103610

Hedin BC, Stuckman MY, Cravotta CA III, Lopano CL, Capo RC (2024) Determination and prediction of micro scale rare earth element geochemical associations in mine drainage treatment wastes: Chemosphere 346:140475. https://doi.org/10.1016/j.chemosphere.2023.140475

Hermassi M, Granados M, Valderrama C, Ayora C, Cortina JL (2022) Recovery of rare earth elements from acidic mine waters: An unknown secondary resource. Sci Tot Environ 810:152258. https://doi.org/10.1016/j.scitotenv.2021.152258

Josso P, Roberts S, Teagle DAH, Pourret O, Herrington R, Ponce de Leon Albarran C (2018). Extraction and separation of rare earth elements from hydrothermal metalliferous sediments. Min Eng 118:106-121. https://doi.org/10.1016/j.mineng.2017.12.014

Karamalidis AK, Dzombak DA (2010) Surface complexation modeling: Gibbsite. John Wiley & Sons, Inc., Hoboken, NJ, USA.

Leon R, Macias F, Canovas CR, Perez-Lopez R, Ayora C, Nieto JM, Olias M (2021) Mine waters as a secondary source of rare earth elements worldwide: The case of the Iberian Pyrite Belt. J Geoch Explor 224:106742. https://doi.org/10.1016/j.gexplo.2021.106742

Liu H, Pourret O, Guo H, Bonhoure J (2017) Rare earth elements sorption to iron oxyhydroxide: Model development and application to groundwater. Appl Geochem 87:158-166. https://doi.org/10.1016/j.apgeochem.2017.10.020

Lozano A, Ayora C, Fernández-Martínez A (2019) Sorption of rare earth elements onto basaluminite: The role of sulfate and pH. Geochim Cosmochim Acta 258:50-62.

Mwewa B, Tadie M, Ndlovu S, Simate GS, Mitinde E (2022) Recovery of rare earth elements from acid mine drainage: A review of the extraction methods. J Environ Chem Eng 10:107704.

Nassar NT, Brainard J, Gulley A, Manley R, Matos G, Lederer G, Bird LR, Pineault D, Alonso E, Gambogi J, Fortier SM (2020) Evaluating the mineral commodity supply risk of the U.S. manufacturing sector. Sci Adv 6:eaay8647. https://doi.org/10.1126/sciadv.aay8647

Nordstrom DK (2020) Geochemical modeling of iron and aluminum precipitation during mixing and neutralization of acid mine drainage. Minerals 10:547. https://doi.org/10.3390/min10060547

Office of Surface Mining Reclamation and Enforcement (2022) AMDTreat 6.0 Beta. https://www.osmre.gov/programs/reclaiming-abandoned-mine-lands/amdtreat

Parkhurst DL, Appelo CAJ (2013) Description of input and examples for PHREEQC version 3—A computer program for speciation, batch-reaction, one-dimensional transport, and inverse geochemical calculations. US Geol Surv Tech Methods 6-A43. https://doi.org/10.3133/tm6A43

Pourret O, Davranche M (2013) Rare earth element sorption onto hydrous manganese oxide: a modeling study. J Colloid Interface Sci 395:18-23. https://doi.org/10.1016/j.jcis.2012.11.054

Royer-Lavallée A, Neculita CM, Coudert L (2020) Removal and potential recovery of rare earth elements from mine water. J Indust Chem Eng 89:47-57. https://doi.org/10.1016/j.jiec.2020.06.010

Rushworth DD, Cravotta CA III, Boyanova MI, O'Loughlin EJ, Kemner KM, Chan CS (2023) Developing an iron biomineral method for sustainable rare earth recovery from acid mine drainage. Am Geophys Union Annual Meeting, Abstract B11G-1874. https://agu.confex.com/agu/fm23/meetingapp.cgi/Paper/1357758

Schulz KJ, DeYoung JH Jr., Seal RR II, Bradley DC, eds. (2017) Critical mineral resources of the United States—Economic and environmental geology and prospects for future supply: US Geol Surv Prof Paper 1802. https://doi.org/10.3133/pp1802I

Swedlund PJ, Webster JG (2001) Cu and Zn ternary surface complex formation with SO4 on ferrihydrite and schwertmannite. Appl Geochem 16:503-511. https://doi.org/10.1016/S0883-2927(00)00044-5

Swedlund PJ, Webster, JG, Miskelly GM (2003) The effect of SO4 on the ferrihydrite adsorption of Co, Pb and Cd ternary complexes and site heterogeneity. Appl Geochem 18:1671-1689. https://doi.org/10.1016/S0883-2927(03)00082-9

Tonkin JW, Balistrieri LS, Murray JW (2004) Modeling sorption of divalent metal cations on hydrous manganese oxide using the diffuse double layer model. Appl Geochem 19:29-53. https://doi.org/10.1016/S0883-2927(03)00115-X

Vass CR, Noble A, Ziemkiewicz PF (2019a) The occurrence and concentration of rare earth elements in acid mine drainage and treatment byproducts: Part 1—Initial survey of the northern Appalachian coal basin. Mining Metal Explor 36:903-916. https://doi.org/10.1007/s42461-019-0097-z

Vass CR, Noble A, Ziemkiewicz P (2019b) The occurrence and concentration of rare earth elements in acid mine drainage and treatment byproducts. Part 2—regional survey of northern and central Appalachian coal basins. Mining Metal Explor 36:917-929. https://doi.org/10.1007/s42461-019-00112-9

Verplanck PL, Nordstrom DK, Taylor HE, Kimball BA (2004) Rare earth element partitioning between hydrous ferric oxides and acid mine water during iron oxidation. Appl Geochem 19:1339-1354. https://doi.org/10.1016/j.apgeochem.2004.01.016

Wang Y, Ziemkiewicz P, Noble A (2021) A hybrid experimental and theoretical approach to optimize recovery of rare earth elements from acid mine drainage precipitates by oxalic acid precipitation. Minerals 12:236. https://doi.org/10.3390/min12020236

Yao W, Millero FJ (1996) Adsorption of phosphate on manganese dioxide in seawater. Environ Sci Tech 30:536-541. https://doi.org/10.1021/ES950290X

Zhang W, Honaker RQ (2018) Rare earth elements recovery using staged precipitation from a leachate generated from coarse coal refuse. Int J Coal Geol 195:189-199. https://doi.org/10.1016/j.coal.2018.06.008

American Chemical Society – Central Regional Meeting
November 6-9, 2024 – Pittsburgh, Pennsylvania

Benchtop assessment of critical metal uptake by hydrous manganese oxide under biotic and abiotic conditions

Tashane J. Boothe-Lordon[1], Rosemary C. Capo[1], Brian W. Stewart[1], Travis A. Olds[2], Carla E. Rosenfeld[2]

[1] *Department of Geology and Environmental Science, University of Pittsburgh, Pittsburgh, PA 15260*
[2]*Carnegie Museum of Natural History, Pittsburgh, PA 15213*

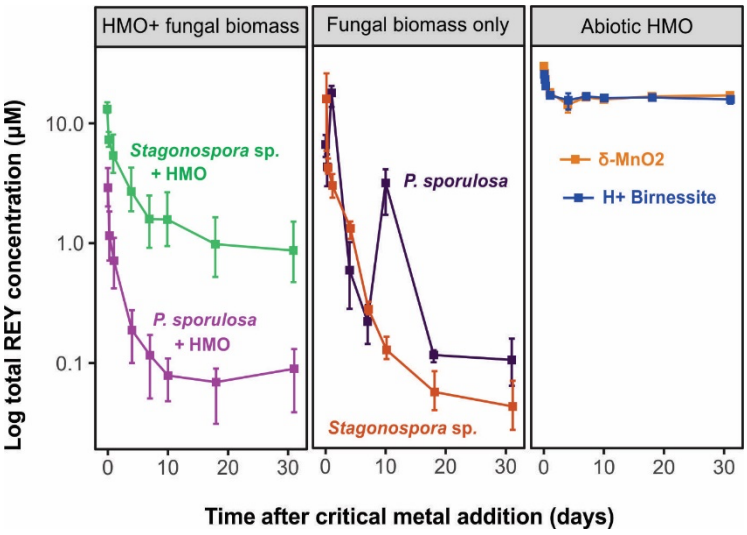

In western Pennsylvania, acid mine drainage (AMD) remediation facilities can produce precipitate byproducts with near ore grade concentrations of REE, Co, and Mn. High concentrations of critical metals in AMD precipitates have been linked to the presence of hydrous manganese oxides (HMO), primarily due to their strong affinity for metals through adsorption and/or coprecipitation. In this study, we investigated the adsorption of 10 critical metals (La, Nd, Ce, Gd, Pr, Dy, Yb, Y, Co, and Ni) from solution by HMO produced by Mn-oxidizing fungi, *P. sporulosa* and *Stagonospora* sp. and HMO (δ-MnO_2 and H+ birnessite) produced by chemical oxidation. Both biotic and abiotic HMO were initially poorly crystalline, but abiotic HMO transformed to more crystalline HMO phases by the end of the experiments. Over 99% of REYs were adsorbed by biotic HMO and/or fungal biomass within 7 days compared to a maximum of 50% of REYs adsorbed by the abiotic HMO. While the adsorption of Co and Ni by abiotic HMO was negligible, biotic HMO adsorbed ~30% Ni and ~75% Co. Microbial biomass did not contribute significantly to adsorption of Co and Ni. This study shows that biotic HMO, which typically form in passive AMD treatment systems, are very efficient at adsorbing critical metals, particularly Co and REE. Fungal biomass may have potential in selectively recovering REY in AMD treatment systems. Abiotic HMO, which are produced in active treatment systems, may be susceptible to mineral transformation and this could reduce their capacity to adsorb some critical metals.

Joint 60th Annual Northeastern/59th Annual North-Central Section Meeting - 2025

Paper No. 45-2
Presentation Time: 1:50 PM

EFFECTS OF SULFATE ON RARE EARTH ELEMENT ADSORPTION AND COPRECIPITATION BY AL HYDROXIDE AND HYDROXYSULFATE PHASES: BATCH EXPERIMENTS AND EQUILIBRIUM MODELS

BOOTHE-LORDON, Tashane[1], CRAVOTTA III, Charles, B.A. Environmental Sciences, Ph.D. Geochemistry and Mineralogy[2], STEWART, Brian[1], CAPO, Rosemary C.[1] and HEDIN, Benjamin[3], (1)Department of Geology and Environmental Science, University of Pittsburgh, Pittsburgh, PA 15260, (2)Cravotta Geochemical Consulting, 859 Bloody Spring Rd, Bethel, PA 19507, (3)Hedin Environmental, 195 Castle Shannon Blvd, Pittsburgh, PA 15228

An understanding of the mechanism(s) of trace metal interactions with acid mine drainage (AMD) solids is needed to develop effective strategies to recover valuable constituents from this unconventional source. In this study, we are investigating the importance of pH and aqueous concentrations of sulfate (SO_4) and aluminum (Al) on the attenuation of rare earth elements (REE) by Al hydroxide and hydroxysulfate phases such as gibbsite ($Al(OH)_3$) and basaluminite ($Al_4SO_4(OH)_{10}.5H_2O$). These phases precipitate within a pH range (4.5-6) that is commonly attained in AMD treatment systems and are important for removing Fe, Al, and trace metals as AMD is neutralized.

We are conducting experiments involving Al precipitation and REE coprecipitation or adsorption from solutions with varying SO_4 concentrations at pH levels relevant to AMD treatment systems. Preliminary modeling of the proposed experimental conditions using PHREEQC indicates that the presence of 10 mM SO_4 results in Al precipitation at a lower pH (4.0-4.5) than in SO_4-free experiments owing to relatively low solubility of basaluminite compared to $Al(OH)_3$. However, when the SO_4 concentration is increased 3-fold, less Al is precipitated at the same low pH value, presumably due to the formation of aqueous complexes with SO_4 which results in a decreased mass of precipitate. For the high-SO_4 scenario, less efficient adsorption of REEs is indicated. Both the availability of sorbent and the potential formation of REE-SO_4-ternary surface complexes explain why REEs are more effectively adsorbed at pH 4.5 in the low-SO_4 solutions compared to the high-SO_4 and SO_4-free solutions. Data from ongoing batch experiments will inform these geochemical models and further elucidate the importance of adsorption and coprecipitation as mechanisms for REE enrichment in Al-rich phases. In addition to simulating empirical data, the modeling will be used to extend results to field conditions and potential scenarios for recovery of REE from AMD treatment systems.

Session No. 45

T27. The Legacy of Coal Mining - Geology, History, Environmental Impacts, and Public Health
Sunday, 30 March 2025: 1:30 PM-5:30 PM

130AB (Bayfront Convention Center)

Geological Society of America *Abstracts with Programs.* Vol. 57, No. 3
doi: 10.1130/abs/2025NE-407795

Appendix B

OSMRE Applied Science Program Fact Sheet

Project Title: Optimizing rare earth element capture during treatment of acid mine drainage: Validation of geochemical modeling through bench-scale experiments and proof-of-concept field studies

Principal Investigator: Dr. Brian W. Stewart, University of Pittsburgh
Co-Principal Investigators:

- Dr. Rosemary C. Capo, University of Pittsburgh
- Dr. Charles A. Cravotta III, USGS (retired), Cravotta Geochemical Consulting
- Benjamin C. Hedin, Hedin Environmental

Project Goals

- Develop scalable methods for extracting rare earth elements and yttrium (REY) from acid mine drainage (AMD)
- Use benchtop experiments and geochemical modeling to optimize REY capture
- Deploy and test a field-based REY-capture system
- Integrate findings into the PHREEQ-N-AMDTreat+REYs geochemical modeling tool

---

Key Findings

- **Modeling & Experiments:**
  - ⇒ Developed predictive geochemical models validated with bench-scale experiments using synthetic and real AMD samples.
  - ⇒ Found optimal pH and sulfate conditions for REY adsorption on hydrous manganese (HMO) and aluminum oxides (HAO).
  - ⇒ Biotic HMO captured >99% of REY, outperforming abiotic HMO.
- **Field Testing:**
  - ⇒ Installed REY capture chambers at two AMD sites along pH gradients.
  - ⇒ Short-term tests indicated growth of HMO on substrate
- **Modeling Tool Release:**
  - ⇒ The PHREEQ-N-AMDTreat+REYs modeling suite, incorporating field and lab data, is publicly available via USGS.

Deliverables

- Final report and summary fact sheet
- Peer-reviewed manuscripts and abstracts
- Technical presentations at national and international conferences
- Public release of PHREEQ-N-AMDTreat+REYs modeling tool

Impacts

- Supports economic and sustainable recovery of REY from AMD
- Offers cost-benefit guidance to AMD treatment operators
- Contributes to national critical mineral supply
- Trains graduate researchers in AMD remediation and geochemical modeling